1973-06

A modified design concept, utilizing deck motion prediction, for the A-7E automatic carrier landing system.

Judd, Thomas Maxwell

Monterey, California. Naval Postgraduate School

A MODIFIED DESIGN CONCEPT, UTILIZING DECK MOTION PREDICTION, FOR THE A-7E AUTOMATIC CARRIER LANDING SYSTEM

Thomas Maxwell Judd

NAVAL POSTGRADUATE SCHOOL
Monterey, California

THESIS

A Modified Design Concept,
Utilizing Deck Motion Prediction,
for the A-7E Automatic Carrier Landing System

by

Thomas Maxwell Judd

Thesis Advisor: Ronald A. Hess

June 1973

Approved for public release; distribution unlimited.

A Modified Design Concept, Utilizing Deck Motion Prediction, for the A-7E Automatic Carrier Landing System

by

Thomas Maxwell Judd
Ensign, United States Navy
B.S.A.E., United States Naval Academy, 1972

Submitted in partial fulfillment of the
requirements for the degree of

MASTER OF SCIENCE IN AERONAUTICAL ENGINEERING

from the

NAVAL POSTGRADUATE SCHOOL
June 1973

ABSTRACT

The present concept of automatic carrier landings, Mode I operational capability, as employed in Navy carrier-based aircraft, was investigated. The aircraft chosen for study was the A-7E. The A-7E All Weather Carrier Landing System (AWCLS) and the carrier landing environment including burble effects and deck motion were simulated. Height of hook above ramp, touchdown point, and velocity of impact dispersions were determined. The current system was then modified, utilizing the concept of a SPN-42 Deck Motion Compensation Lead Computer which operates on the basis of known aircraft characteristics and predicted carrier heave motion. Simulation showed that automatic carrier landing performance as measured by number of ramp strikes, hard landings, and bolters could be improved. The modifications suggested require only a minimum of component additions to the AWCLS currently in use in the Navy.

SYMBOLOGY

ACLS	Automatic Carrier Landing System
AFCS	Automatic Flight Control System
AOA	Angle of attack
APCS	Approach Power Compensator System
AWCLS	All-Weather Carrier Landing System
bolter	Landing on the carrier deck beyond the final wire
c.g.	Center of gravity
c.p.	Center of pressure
CSMP	Continuous System Modeling Program
DMC	Deck Motion Compensation
dB	Decibels
hhc.g.	Aircraft c.g. to hook horizontal distance
hvc.g.	Aircraft c.g. to hook vertical distance
LSO	Landing Signal Officer
MAC	Mean aerodynamic chord
pcalt	Vertical distance from carrier pitch center to ideal touchdown point measured perpendicular to hull centerline
pcang	Angle between carrier pitch center and ideal touchdown point, measured from parallel to hull centerline
pcran	Horizontal distance from pitch center to ideal touchdown point, measured parallel to hull centerline
pcslt	Pitch center to ideal touchdown point actual distance
PLA	Power Lever Angle

rad	Radian
RMS	Root Mean Square
S	Aircraft wing area
s	Laplace transform variable
TD	Ideal touchdown point
U_O	Aircraft inertial velocity (ft/s)
UHF	Ultra high frequency
UHT	Unit Horizontal Tail
WOD	Wind over deck
x_f	Ideal touchdown point to ramp distance, measured parallel to hull centerline
ΔZ_c	Deck Motion Compensation signal
Z_e	Altitude error signal
Z'_e	Altitude error signal minus ΔZ_c
Z_{11}	Washed out measured heave of the ideal touchdown point, positive up
α_0	Body angle of attack of the aircraft
β	ACLS-commanded glide slope angle
θ_c	ACLS-commanded pitch angle
θ_0	Initial approach pitch attitude of the aircraft
θ_s	Measured pitch of the carrier
δ_e	UHT deflection angle
δ'_e	Washed out UHT deflection angle

TABLE OF CONTENTS

LIST OF TABLES

LIST OF FIGURES

ACKNOWLEDGEMENT

The author wishes to thank Assistant Professor Ronald A. Hess for his guidance and assistance throughout the course of this research. This work could also not have been accomplished without the assistance of A-7 pilot Lieutenant David H. Finney, USN; Mr. Robert F. Ringland and Mr. Arthur A. Blauvelt of Systems Technology, Inc., in Hawthorne, California; and Mr. Robert F. Wigginton and Mr. Henry Agnew of the Naval Air Test Center, Patuxent River, Maryland.

The patience and moral support shown by the author's wife, Ann, was greatly appreciated.

I. INTRODUCTION

A. AWCLS PERFORMANCE OBJECTIVES AND DESCRIPTION

The primary purpose of the All-Weather Carrier Landing System (AWCLS) Mode I is to provide fully automatic control of an aircraft from AWCLS entry point to touchdown on the carrier deck. Reference 1 states the performance criteria which must be met. These include landings in zero visibility with a touchdown longitudinal dispersion of $\pm$ 40 feet from the point midway between the #2 and #3 wires on the carrier deck, in sea conditions resulting in deck motion of 1.25 degrees root-mean-square (RMS) pitch, 4 feet RMS heave, and with maximum vertical translation of the ramp of $\pm$ 20 feet. Main hardware components of the longitudinal channel of the AWCLS include the aircraft and the SPN-42. The latter is a shipboard navigational system that uses both radar to determine the aircraft position and a real-time digital computer to generate pitch commands for the aircraft Automatic Flight Control System (AFCS). The pitch commands are generated in part by a digital compensation network which receives an error signal proportional to aircraft deviation from the desired flight path altitude, and in part by a change in flight path altitude occurring when Deck Motion Compensation (DMC) is utilized in the landing process. DMC initiates a change in aircraft altitude because of the changing altitude of the desired touchdown point due to carrier heave. These DMC altitude

commands are summed with the flight path altitude errors to generate pitch command signals, beginning at 12 seconds from touchdown and continuing until frozen at 1.5 seconds from touchdown. The total pitch command, which also includes a tipover command to initially acquire the desired glide slope, is processed by a floating limiter. Utilizing a UHF Data Link, the floating limiter output is transmitted to the aircraft. AWCLS operation requires that the aircraft possess an Approach Power Compensator System (APCS) for maintaining constant angle-of-attack on glide slope, and an AFCS for processing the Data Link pitch commands. The lateral AWCLS channel, which is not considered in this report, is similar to the longitudinal channel but processes bank angle commands that result from measured lateral excursions from the carrier runway centerline.

A typical automatic carrier landing sequence proceeds as follows: the aircraft while flying straight and level aft of the carrier is aligned by the pilot with the deck centerline. Two to four miles aft of the carrier the aircraft passes through the AWCLS acquisition window at which point the SPN-42 transmits a discrete ACL (Automatic Carrier Landing) LOCK-ON signal. When the SPN-42 is ready to assume control, it transmits a COUPLER AVAILABLE discrete signal indicating that the AFCS can be coupled to the Data Link. The pilot performs the coupling and verbally acknowledges the engagement. When transmission of pitch and bank commands is initiated, a COMMAND CONTROL discrete

is transmitted. Three seconds before the aircraft intersects the programmed glide slope the SPN-42 adds the tipover command to the longitudinal compensation network commands. At 12 seconds from touchdown, a discrete is transmitted indicating that DMC commands are now being added to give the desired flight path altitude. Then at 1.5 seconds from touchdown, the Data Link commands are frozen and the AFCS holds the aircraft attitude to touchdown.

Of primary interest is the ability of the existing AWCLS to perform acceptably under the sea/deck conditions as indicated to be necessary in military specifications. Reference 2 states that six separate parameters are needed to describe total landing performance. They are the means and standard deviations of (a) ramp clearance, (b) impact velocity, and (c) touchdown distance. Total performance of competing systems is ultimately determined by relating the six measures of performance stated above to accident rate and bolter rate.

B. AIRCRAFT

The aircraft chosen for study was the A-7E, a single-place light attack, carrier and land-based aircraft of approximately 20,000 pounds empty gross weight. The A-7E was chosen because of the availability of information on its existing AWCLS components and Mode I operational capability [Ref. 3], information on its aerodynamic characteristics [Ref. 4] and the availability of verbal inputs from experienced A-7 pilots at the Naval Postgraduate School.

The A-7E powerplant is an Allison TF41-A-2 turbofan engine whose throttle response is characterized by a relatively large and nonlinear time constant in the approach thrust range. Longitudinal control is provided by a movable unit horizontal stabilizer.

C. CARRIER

To provide a realistic simulation, carrier geometry corresponding to the USS ENTERPRISE (CVA(N)-65) was obtained. ENTERPRISE was chosen because of the availability of its plan view and because pitch center information was available in Reference 5. Basically ramp-to-ideal touchdown point distance, ramp-to-pitch center angle and distance, and touchdown point-to-pitch center angle and distance were utilized.

D. PREVIOUS STUDIES

Naval Air Test Center, Patuxent River, Maryland, conducted an evaluation of A-7E ACLS Mode I operation and attempted to determine if a single mode APCS would be compatible with both ACLS and manual control [Ref. 3]. The following is a summary of pertinent conclusions and recommendations:

1. Mode I ACLS performance is feasible with the A-7E airplane equipped with the "Dash 6" APCS computer within certain operational limitations on deck motion, wind over deck, and weather minimums.

2. A-7E Mode I operations should be restricted to deck motion limits of 1.5 degrees peak-to-peak ship pitch and 6 feet peak-to-peak touchdown point heave, and wind-over-Deck (WOD) limits of 345 degrees to 005 degrees relative between 18 knots and 40 knots.

3. For ACLS control of the A-7E airplane when WOD exceeds 25 knots, a basic glideslope angle of 4.0 degrees should be utilized; for ACLS control when WOD is less than 25 knots, a basic angle of 3.5 degrees should be utilized.

Systems Technology, Incorporated (STI) has made an analysis of the carrier landing environment to provide an analytic base useful in the development of improved carrier landing methods and systems [Ref. 2]. From this study, methods for determining terminal landing errors and resulting operational performance indices are presented. Also, the possible uses of predicted deck position and contingent minimum prediction time and accuracy requirements are considered. The following is a summary of pertinent conclusions and recommendations:

1. A minimum prediction time of five seconds is required from a deck motion predictor for it to be useful, with a minimum accuracy requirement that the predictor reduce the uncertainty of deck position at touchdown by at least a factor of two over the no prediction case, that is, RMS prediction errors must be less than 50 per cent of the actual RMS deck motion.

2. This minimum capability predictor is seen to have two immediate uses, providing inputs to a waveoff computer and biasing the Fresnel lens system to compensate for high ramp conditions.

3. For prediction to be useful regarding the reduction of accidents, a performance level exceeding the nominal Landing Signal Officer (LSO) performance should be realized. STI's study indicates that LSO action reduces the unsafe-pass probability of aircraft by a magnitude of ten over the no-prediction case. However, this figure of 90 per cent "saves" attributed to LSO action is representative of average recovery conditions, and is of doubtful validity when considering severe deck pitching conditions and accompanying turbulence. Also, the 90 per cent "save" assessment will probably not be met in the situation where the number of passes

to safely land becomes critical, and because fuel state is low and the pilot has received one or more waveoffs, the LSO will tend to become less critical in subsequent passes. Prediction could be very helpful in such a situation.

STI has also studied the concept of a SPN-42 DMC Lead Computer. In an unsolicited technical proposal, [Ref. 6], measurement and utilization of deck motion prediction time is presented. The proposal states the following:

> The SPN-42 . . . (ACLS) deck motion compensation mode is designed to increase the probability of a successful landing in the presence of deck motion by commanding the aircraft to chase the touchdown point. Because of the inevitable time lags between command and aircraft response, it is necessary for this command to lead the deck position, the amount of lead required depending on the response of the airplane/AFCS system. Presently the SPN-42 uses a second-order filter for this purpose, and obtains from the filter about 1.7 seconds of approximate lead (considered appropriate to F-4 response properties) on its DMC command. Attempting to increase the amount of lead generated by this filter would significantly increase its errors . . . since a second order filter (or feed forward) is limited in its ability to get a proper lead for an input that is not a single frequency but a narrow banded random process such as ship's motion. For a conventional feed forward, thus limited to approximately 1.7 seconds, the corresponding required airplane/autopilot response may be difficult to obtain for some aircraft (notably the A-7) without incurring objectionable pitch overshoot or other symptoms of marginal stability.
>
> Rather than attempting to increase the altitude response of the aircraft, a preferable solution would be to increase the capability of the feed-forward. For example, if the feed-forward lead could be increased to 3 or 4 seconds, then the frequency response characteristics of the aircraft/SPN-42 loop closure could be considerably reduced. The advantage of this would be a reduction in the structural loads placed on the aircraft, an increase in the stability of the SPN-42/aircraft loop, and a reduction in the autothrottle requirements. A further possible advantage could be a reduction in the sensitivity of the aircraft/SPN-42 loop to gusting effects.

Based on the preceding considerations, STI proposed a heave lead computer capable of generati ng a signal leading the vertical displacement of the touchdown point by 2 to 4.5 seconds, the value selected by the SPN-42 system dependent on aircraft under automatic control. Implementation of such a lead-time computer would create a situation of nearly zero phase lag between deck motion and altitude response to this motion, that is, in the "deck-chase" mode of the AWCLS Mode I, the aircraft would follow ship heave motion almost perfectly.

E. OBJECTIVES

The purpose of this research was to improve the performance of the current AWCLS concept as implemented in the A-7E aircraft. Specifically, the effect of utilizing deck heave prediction to generate sufficient lead to meet the A-7E altitude response lag was evaluated. By decreasing dispersions associated with ideal touchdown point landing, ramp clearance, and velocity of impact, which in turn will yield decreased accident and bolter rates, the degree of improved performance was determined.

II. METHOD OF ANALYSIS

A. DESCRIPTION OF THE MODEL

1. Introduction

The fully automatic carrier landing mode (MODE I), utilizing the current operational concept of the A-7E AWCLS longitudinal channel, served as the baseline configuration in this analysis. Also modeled was a modified baseline configuration, with deck motion predictor information used to provide nearly zero phase lag between deck heave and A-7E altitude response. Based on performance indices which could be reduced to number of accidents and bolters, the two systems were open to comparison. In both configurations, the total closed loop system consisted of the airframe, the engine, the approach power compensator, the longitudinal flight control system (AFCS), the automatic carrier landing system (ACLS), and parameters associated with the deck motion and carrier landing environment.

2. Aircraft Model

The aircraft equations of motion were linearized about the steady state (on glide slope) approach conditions in accordance with standard small perturbation theory, as described by Etkin [Ref. 7]. Lateral-directional dynamics were not included. The resultant equations are shown in Figure 1. Aircraft stability derivatives and

other parameter values were taken from Ref. 4 and are listed in Table I. Force and moment stability derivatives are normalized with respect to mass and moment of inertia, respectively. Hence mass and moment of inertia do not appear explicitly in the equations of motion, as they do in Etkin's notation.

The A-7E engine is the TF41-A-2 turbofan. Reference 8 contains an analysis of the thrust-power lever relationship for a range of operating conditions. The nominal approach thrust for the operating conditions as shown in Table I is 3000 pounds. In this range of thrust, the engine response time constant is a nonlinear function of thrust. The relationship between the engine time constant, T_e, and thrust, and the relationship between thrust and power lever angle (δ PLA) for the given operating conditions are taken from Ref. 4, and are shown in Figure 2. An average value of 275 pounds thrust per degree δ PLA was used in the model. Thus, the variable engine lag was the only non-linearity in the engine model.

Figure 3 is a schematic of the APCS loop closures. In small perturbation theory, angle-of-attack (AOA) is defined as w/U_0, in radians. Thus, the inputs to the APCS computer are proportional plus integral w, a_z' (vertical acceleration corrected for accelerometer location), and a filtered Unit Horizontal Tail (UHT) feed forward term.

The APCS gains are from the Dash 6.12 computer which, according to Agnew [Ref. 9], is the current A-7E APCS configuration. However, several simplifications were made to the APCS model. A

complex pole at ten radians per second in the throttle actuator response was neglected. This frequency is well beyond the range in which the APCS is effective. Throttle linkage hysteresis of 0.5 degrees was ignored. A gain-adjust bias exists in the APCS which changes all APCS gains by the same amount to compensate for ambient air temperature effects. The standard day value of 1.0 was used. K_{n_z}, the vertical acceleration gain, has two values, the smaller value being for load factors in excess of 1.1 g's. Only the larger value was incorporated into the model. A dual time constant in the UHT crossfeed circuit which uses a shorter time constant for nose-up corrections than for nose-down corrections, has been shown to greatly improve APCS performance. It is currently in use in the operational aircraft and is modeled in the program.

Both the longitudinal AFCS and the ACLS models were taken from Ref. 10, and represent the current operational concept. A complex pole and a first order lag at 20 radians per second in the AFCS response were neglected. The AFCS output is a UHT deflection, which is a function of attitude error $(\theta-\theta_c)$, pitch rate, and normal acceleration. The automatic carrier landing system was represented by the A-7E SPN-42 longitudinal control equation. The output, a ship-to-aircraft pitch command, is a function of the aircraft altitude error, $\dot{Z}_e$. This in turn, is a function of the aircraft's distance from the ideal glide slope, a ramp bias term due to ship's RMS pitch, and deck motion compensation, when employed. In practice, the aircraft slant

range and elevation are measured by the SPN-42 radar, corrected for ship motion and radar location, transformed into cartesian coordinates and utilized to command aircraft pitch angle. The AFCS and ACLS longitudinal control equations are shown in Figure 4. APCS, AFCS, and ACLS gains are listed in Table II.

3. Carrier Model

Reference 2 states that motion of a carrier deck results from the ship's response to sea wave and swell wave excitations. This motion, in turn, affects the generation of deck motion compensation, when employed, and glide slope angle bias and altitude bias terms which make allowances for vertical translation of the carrier ramp. Thus, deck motion contributes directly and indirectly to terminal dispersions in aircraft height-above-ramp, touchdown point, and velocity of impact. The result of the wave input acting through the ship's dynamic characteristics may be represented with power spectral densities of ship's pitch, heave, and roll, giving a clear indication of deck motion dominant frequencies. From Figure 5 it may be seen that both heave frequencies and pitch frequencies are dominant in the range from 0.45 to 0.75 radians per second. In the dominant frequency region of the ship motion power spectra, pitch leads heave by 45 to 90 degrees. A complete phase angle relationship is presented in Ref. 11. For simplicity, pitch was assumed to lead heave by 90 degrees in this simulation. As stated in Ref. 2, RMS values of pitch and heave of 1.0 degree and 5.5 feet, respectively,

correspond to upper limits for normal aircraft launch and recovery operations sea conditions. Moderate sea state conditions as defined by Ref. 12 include $\pm$ 4 feet of heave and $\pm$ 0.75 degrees of pitch. Assuming sinusoidal deck heave and pitch, the simulations utilized 1.0 degree and 0.5 degrees RMS pitch (corresponding to $\pm$ 1.4142 degrees and $\pm$ 0.7071 degrees pitch), $\pm$ 4 feet and $\pm$ 8 feet heave, and a dominant frequency of 0.60 radians per second.

At the time of AWCLS coupling to the UHF Data Link, measured ship's pitch determines the aircraft glide slope angle. RMS pitch of 0.5 degrees or less (moderate sea conditions) will result in a glide slope of 3.5 degrees. For RMS pitch up to 1.0 degree, the glide slope angle is incremented until a maximum glide slope of 4.5 degrees is set for pitch greater than or equal to the 1.0 degree RMS value. Also, an altitude bias term, represented by 0.5 times the product of pitch and ideal touchdown point-to-ramp distance, is added to the altitude error to result in a greater ship-to-aircraft attitude command and thus, combined with the glide slope angle bias, the added insurance of a few feet higher trajectory above the pitching carrier ramp.

A realistic carrier landing will normally be accomplished only after contending with the effects of the "burble" behind the carrier ramp. Reference 2 surveys the work done by Oceanics, Inc., and the David Taylor Model Basin (DTMB) in identifying and qualitatively describing the three air wake components: steady-state burble, pitch-induced wake, and random turbulence. From this combined Oceanics/

DTMB data, BURBLE Model No. 1 [Ref. 13] was synthesized, showing extremes in the correlated data, that is, the maximum burble effects. This model consists of horizontal and vertical gust velocities with the latter exhibiting either an updraft-downdraft pattern or a downdraft-updraft pattern. BURBLE Model No. 1 is shown in Figure 6.

B. DIGITAL SIMULATION

1. Continuous System Modeling Program

The closed loop system was simulated on the IBM 360 digital computer utilizing a digital simulation language, CSMP. CSMP is an acronym for Continuous System Modeling Program. The program is augmented by basic Fortran and provides a set of functional blocks which simulate such analog components as integrators, relays, and function generators. A detailed description of the program is contained in Ref. 14. A description of CSMP functions used in the simulation is provided in Table III.

2. CSMP Program Components

A sample program and output are contained in Appendix A. The program consists of seven major sections: the simulation nonlinearities, parameters, and initial conditions section, the aircraft equations of motion and engine model, the ship pitching motion input and resulting parameters section, the ACLS and deck motion compensation model, the AFCS model, the APCS model, and the carrier approach profile.

a. Simulation Nonlinearities, Parameters, and Initial Conditions

(1) Thrust versus engine time constant, a nonlinear curve, was approximated using the CSMP linear function generator option.

(2) The BURBLE Model No. 1 was also approximated using the linear function generator option.

(3) Input parameters included such values as deck motion amplitudes and frequency, carrier geometry, and aircraft geometry.

(4) Initial conditions included such values as initial aircraft range, altitude, and glide slope angle.

b. Aircraft Equations of Motion and Engine Model

The equations of motion as shown in Figure 1 were put into state variable format:

$$\begin{aligned} \{\dot{X}\} &= [A]\{X\} + [B]\{R\} \\ \{\dot{Y}\} &= [C]\{X\} + [D]\{R\} + [E]\{Y\} \end{aligned} \tag{1}$$

where

$$\{X\} = \begin{Bmatrix} u \\ w \\ \theta \\ q \end{Bmatrix} \qquad \{Y\} = \begin{Bmatrix} \dot{h} \\ a_z \\ a_z' \end{Bmatrix} \qquad \{R\} = \begin{Bmatrix} \delta_e \\ \Delta_T \\ u_g \\ w_g \end{Bmatrix} \tag{2}$$

The A, B, C, D, and E matrices are listed in Table IV.

The engine modeling consisted of two parts. As mentioned in Section II.A., a relationship of 275 pounds thrust per degree δPLA was assumed. The thrust operating range modeled in

part a. of this section was ± 2000 pounds about the nominal operating value of 3000 pounds.

c. Ship Pitching Motion Input and Resulting Parameters

(1) RMS ship pitching motion is input at the same frequency as ship heaving motion with a 90 degree lead in phase.

(2) Resulting parameters include pitch-induced vertical translation of the touchdown point and the ramp bias term due to ship's RMS pitch.

d. ACLS and Deck Motion Compensation Model

The altitude, Z_e, was previously defined to be a combination of three inputs: the negative of h (the two are measured in opposite directions perpendicular to the ideal glideslope), the ramp bias term due to ship's pitch, and a deck motion compensation term when employed. The θ_c/Z_e transfer function, called the F-5 program and currently in use in the Navy aboard USS J. F. KENNEDY and USS CORAL SEA, is shown in Figure 4 and was rearranged for programming as follows:

$$\frac{\theta_c}{Z_e} = \frac{K_c K_x}{K_p s+1} \left(\frac{\frac{s}{3.9} + 1}{\left(\frac{s}{5}\right)^2 + \frac{s}{3.5} + 1} \right) \left(\frac{t_i K_x}{s} + 1 \right) + \left(\frac{s R_0}{\left(\frac{s}{5}\right)^2 + \frac{s}{3.5} + 1} \right) X$$

$$\left(\frac{t_a s}{(K_a s+1)^2} + t_R \right)$$

$$= \frac{K_0}{s} \cdot \frac{s^4 + b_3 s^3 + b_2 s^2 + b_1 s = b_0}{s^5 + a_4 s^4 + a_3 s^3 + a_2 s^2 + a_1 s + a_0} = \frac{Z_i \theta_c}{Z_e Z_i} \qquad (3)$$

where:

$$K_0 = \left(\frac{25\ K_c K_x}{(3.9)\ (57.296)} \right) \left(\frac{3.9\ R_0 t_r + 1}{K_p} \right)$$

$$a_4 = \frac{(K_a)^2 \left(\frac{25}{3.5}\ K_p + 1\right) + 2\ K_a K_p}{(K_a)^2\ K_p}$$

$$a_3 = \frac{(K_a)^2 \left(25\ K_p + \frac{25}{3.5}\right) + \frac{50}{3.5}\ K_a K_p + 2\ K_a + K_p}{(K_a)^2\ K_p}$$

$$a_2 = \frac{25\ (K_a)^2 + 50\ K_a K_p + \frac{50}{3.5}\ K_a + \frac{25}{3.5}\ K_p + 1}{(K_a)^2\ K_p}$$

$$a_1 = \frac{50\ K_a + 25\ K_p + \frac{25}{3.5}}{(K_a)^2\ K_p}$$

$$a_0 = 25.0$$

$$b_3 = \frac{(K_a)^2\ (t_i K_x + 3.9) + 2\ K_a\ (3.9\ R_0 t_R + 1) + 3.9\ R_0 t_a}{b_6}$$

$$b_2 = \frac{(K_a)^2\ (3.9 t_i K_x) + 2\ K_a (t_i K_x + 3.9) + (3.9\ R_0 t_R + 1)}{b_6}$$

$$b_1 = \frac{2 K_a (3.9 t_i K_x) + (t_i K_x + 3.9)}{b_6}$$

$$b_0 = \frac{3.9 t_i K_x}{b_6}$$

$$b_6 = (K_a)^2 (3.9 R_0 t_R + 1)$$

The SPN-42 equations in the simulation are in the form of the right side of Equation (3).

When deck motion compensation is introduced 12 seconds prior to touchdown, it is done so gradually, over a two-second period, increasing from zero to full compensation. This is simulated, utilizing the CSMP 'Macro' option, by having no compensation prior to the 12-second point, one-half compensation at the 11-second point, and full compensation at the 10-second point. The DMC input ΔZ_c is computed on the basis of the measured heave (Z_{11}) of the carrier at the ideal touchdown point. The $\Delta Z_c / Z_{11}$ transfer function, as shown in Figure 4, was rearranged for programming as follows:

$$\frac{\Delta Z_c}{Z_{11}} = K \cdot \frac{K_1 s^2 + K_2 s + 1}{(T_1 s + 1)^3} \cdot \frac{K_3 s + 1}{T_2 s + 1} \qquad (4)$$

$$= C_6 \cdot \frac{s^2 + D_1 s + D_0}{s^3 + C_2 s^2 + C_1 s + C_0} \cdot \frac{K_3 s + 1}{T_2 s + 1} = \frac{Z_d}{Z_{11}} \frac{Z}{Z_d} \frac{\Delta Z_c}{Z} \qquad (5)$$

where:

$$C_6 = \frac{K \cdot K_1}{(T_1)^3} \qquad C_2 = \frac{3}{T_1} \qquad C_1 = \frac{3}{(T_1)^2}$$

$$C_0 = \frac{1}{(T_1)^3} \qquad D_1 = \frac{K_2}{K_1} \qquad D_0 = \frac{1}{K_1}$$

The DMC equations in the simulation are in the form of the right side of Equation (5).

e. AFCS Model

The AFCS equations were obtained from the equation given in Figure 4 with numerical values substituted for the various gains. The gains, as given in Table II are those in current operational usage.

f. APCS Model

The APCS equations were obtained from Figure 3. The throttle actuator, power lever, and engine gains were combined into a single parameter. As a result, the variable labeled "PLA" in the CSMP program is not the actual power lever angle. Gains and other constants were also consolidated whenever possible. AOA and integral of AOA were kept distinct. For ease of programming, the δ_e' / δ_e transfer function was written as the following:

$$\frac{\delta_e'}{\delta_e}(s) = \frac{K_{\delta_e} T_w s}{T_w s + 1} = \frac{1}{s + 1/T_w} \cdot K_{\delta_e} s = \frac{W_1}{\delta_e} \cdot \frac{\delta_e'}{W_1} \qquad (6)$$

The UHT input equations in the simulation are in the form of the right side of Equation (6). Utilizing the 'Procedure' option of CSMP, the dual time constant of the UHT crossfeed circuit was modeled.

g. Carrier Approach Profile

Carrier altitude and range with respect to the ideal touchdown point were determined by integration of the linearized kinematic equations from Etkin [Ref. 7]. The carrier ramp-crossing time and the height of aircraft hook above the ramp were determined, as were the time of the main gear touchdown, the position of the landing on the deck with respect to the ideal touchdown point, and the velocity of impact associated with that landing. The manner in which they were determined is shown in Appendix B. Velocity of impact was defined as the linear combination of aircraft sink rate and vertical velocity of the carrier's ideal touchdown point. The vertical velocity of the carrier's ideal touchdown point was measured using the 'Derivative' option of the CSMP program package, and equalled the derivative of vertical translation of the touchdown point due to ship's pitch and heave.

III. PROCEDURE

A. DIGITAL SIMULATION RUNS

A standard set of runs for the digital simulation was utilized for the baseline AWCLS model and the modified AWCLS model utilizing deck motion prediction. The length of the simulation runs was chosen to approximate the final approach phase of the carrier landing. Under SPN-42 control, two of the ACLS equation gains, R_0 and K_x, are functions of range. For ranges in use in this simulation of less than 7000 feet, R_0 remains constant at the value shown in Table II. K_x, however, changes in this range area of interest, and was modeled using the CSMP 'Procedure' option to provide the correct value for the current range. K_x values are also shown in Table II. A run time of 33 seconds was chosen to approximate this phase of the approach. Initial range and altitude were set up, assuming ideal touchdown would occur in 30 seconds. A fourth order Runge-Kutta integration technique was used, with fixed step size of 0.05 seconds. Two standard runs were set up for each configuration, one using the updraft-downdraft burble model, and the other using the downdraft-updraft burble. In each, height of hook above ramp, touchdown position, and velocity of impact were measured at two combinations of pitch and heave amplitude and frequency. In simulating deck pitch and heave at moderate and severe sea conditions, the two deck motions were assumed to occur at the same frequency.

B. ANALYSES OF THE BASELINE AND MODIFIED BASELINE AWCLS CONFIGURATIONS

When the AWCLS goes into its deck-chasing mode, Z_{11}, the measured vertical motion of the ideal touchdown point, is passed through the digital equivalent of a phase lead network to create ΔZ_c. Ideally, this compensation would counteract the lag of the SPN-42/aircraft servomechanism system. The form of the current lead network transfer function is a third-order polynomial in 's' divided by a fourth-order. The constant terms in this transfer function are tuned to the particular aircraft type to represent the inverse of the SPN-42/aircraft altitude response within $\pm$ 1 dB in gain, $\pm$ 15 deg of phase in the frequency range out to 1 rad/s.

An approach contrary to the preceding for providing in-phase compensation was made in this simulation. From baseline configuration digital output, phase difference for the deck heave input and the resultant aircraft altitude response was measured to be approximately 1.1 seconds. This means that the A-7E SPN-42/aircraft servomechanism lag is approximately 2.8 seconds, recalling that the current lead network provides 1.7 seconds deck heave prediction. For the modified baseline configuration, therefore, assuming that the STI DMC Lead Computer could provide a feed-forward of 2.8 seconds, the heave input to the DMC transfer function was advanced 1.1 seconds. The assumption of purely sinusoidal heave motion at one dominant frequency made the changeover from the baseline to modified baseline configuration a simple one, as shown below:

Baseline input to DMC Transfer function (1)

Z_{11} = Heave Amplitude X sin (Heave Frequency X Time + Phase Angle)

Modified Baseline input to DMC transfer function (2)

Z_{11} = Heave Amplitude X sin (Heave Frequency X (Time + 1.10) + Phase Angle)

A term, Z_{12}, was defined in the simulation to be equal to Equation (1) above. This term was used in both configurations in the determination of ramp and landing dispersions.

IV. DISCUSSION AND RESULTS

A. INTRODUCTION

Initial digital runs were made to determine the approach and landing parameters for the no-burble, no pitch and heave case, and the no-burble, severe sea conditions' pitch and heave cases for the baseline and modified baseline configurations. The following are the results:

Case (1)

Burble	Height above Ramp	Landing Position	Impact Velocity
None no pitch and heave	11.5567 ft	-5.0117 ft	13.3071 ft/s

Case (2)

None severe pitch and heave	12.9094 ft	83.8555 ft	19.7681 ft/s

Case (3)

None severe pitch and heave	12.5746 ft	41.4180 ft	14.6316 ft/s

The landing position shown in case (1) results from the fact that the glide slope was set up so that the main gear of the aircraft would reach within $\pm$ 1 foot of zero altitude at the end of 30 seconds and at

the ideal touchdown point. Case (3) shows improvement in two aspects over Case (2). Landing position is achieved closer to the ideal, and velocity of impact is decreased significantly.

Comparison of the baseline configuration with the modified baseline configuration will be restricted to the cases where the updraft-downdraft burble pattern is utilized. Occurrence of this burble pattern is more likely in a realistic carrier landing environment. Results from simulation using the downdraft-updraft burble pattern generally showed the tendency of the aircraft to bolter. The aircraft's reaction to the downdraft effects were to generate a pitch-up command. This reaction, in combination with the ensuing updraft and freezing of the pitch command at 1.5 seconds prior to touchdown, led to the situation where the aircraft was high at the ramp in a higher than normal pitch attitude. It is noted that 10 landings in 36 attempts were achieved by the baseline configuration in which the aircraft's altitude response was not in phase with ship's heave. No landings were achieved with the modified baseline configuration.

B. BASELINE AWCLS CONFIGURATION

The means and standard deviations of height of hook above ramp, touchdown position, and velocity of impact, with simulated severe deck motion conditions, were the following for the baseline configuration data shown in Table V.

Burble Updraft-downdraft	Height above Ramp (ft)	Landing Position (ft)	Impact Velocity (ft/s)
Mean	16.499	22.763	20.905
Standard Deviation	8.270	75.849	6.007

For this configuration, the 36 landings involved incurred 12 ramp strikes, 15 hard landings, and 2 bolters. The relatively large number of ramp strikes is due to the prolonged effect of the downdraft in the burble, causing the aircraft to be low at the ramp. The mean landing position for those paths not involving a ramp strike reflected meeting of military specifications of $\pm$ 40 feet around the ideal touchdown point, but was actually accomplished in only 9 of the landings. The 15 hard landings that were recorded, in which the aircraft structural limits set at 23 feet per second were exceeded, were generally due to the added velocity of the burble and the pitching angle of the carrier deck.

It is clear, in terms of potential accidents, that the combination of severe sea condition-induced deck pitch and heave with the updraft-downdraft burble pattern can yield the most dangerous carrier landing situation. It is noted here that the current AWCLS lessens the effect of the low ramp situation by introducing an error ramp and a command ramp as shown in Figure 7. The error ramp raises the vertical reference of the aircraft to counteract the settling effect of the aircraft as it passes through the burble. Command ramp is a fly-up command added to the total aircraft pitch command, for the purpose of providing

a slight increase in the aircraft's power as it nears touchdown in an effort to overcome the effects of air turbulence. Both the command ramp and the error ramp are functions of the ship and aircraft type. The currently used values were not available and were neglected in modeling the baseline configuration. Further description of the command and error ramps is available in Ref. 15.

The problem of ramp strikes should theoretically be eliminated by utilizing deck heave prediction, which would synchronize the aircraft altitude response with the heave. With the inclusion of the RMS pitch-dependent glide slope bias and the ramp bias, the aircraft hook should clear the ramp.

C. MODIFIED BASELINE AWCLS CONFIGURATION

1. Severe Sea Conditions

Simulation of the modified baseline configuration with severe deck motion conditions, utilizing deck heave prediction, yielded the following results, determined from the data shown in Table VI.

Case (1)

Burble Updraft-downdraft	Height above Ramp (ft)	Landing Position (ft)	Impact Velocity (ft/s)
Mean	10.497	77.076	18.866
Standard Deviation	6.464	53.868	4.971

Case (2)

Updraft-downdraft			
Mean	14.503	12.961	16.389
Standard Deviation	6.966	58.142	6.124

For the modified configuration of Case (1), the 36 landings involved generated 4 ramp strikes, 9 hard landings, and no bolters. The extreme effects of the burble pattern to some extent compromised the effectiveness of the heave prediction. However, the effect of tighter glide path control may be seen with a significantly reduced landing position standard deviation, with respect to the baseline configuration. Improvement was also noted by the increased number of landings meeting military specifications (12), and reduced number of hard landings. The critical reduction of ramp strikes by the modified configuration was further augmented by the input of an error ramp. The addition of 6 feet to the aircraft vertical reference eliminated all ramp strikes and otherwise achieved the results as shown in Case (2) above. The data for Case (2) is presented in Table VII. The addition of the error ramp resulted in 5 bolters, 7 hard landings, and 14 landings meeting military specifications. Case (2) was simulated to show how a typical error ramp could improve approach and landing parameters, utilizing the advantage of deck heave prediction.

2. Moderate Sea Conditions

Burble Updraft-downdraft	Height above Ramp (ft)	Landing Position (ft)	Impact Velocity (ft/s)
Mean	5.203	117.234	15.234
Standard Deviation	3.049	34.160	2.269

The moderate sea condition carrier environment was modeled to determine limiting sea conditions for which the modified AWCLS configuration could be used, without incurring hard landings. Because BURBLE Model No. 1 is representative of severe sea conditions-induced burble, it has a dominating effect on landing position for the configuration in this section, as evidenced by the mean landing position being well short of the #1 wire on the carrier deck. However, an indication of sea conditions limits which are plausible for safe AWCLS operation can be determined by comparing means and standard deviations of impact velocities between the moderate and severe modified baseline configurations. From this comparison, approximate limits of 7 feet of deck heave and 1.2 degrees of ship's pitch were determined. Data for this configuration is shown in Table VIII.

V. CONCLUSIONS AND RECOMMENDATIONS

A. AWCLS CONFIGURATION

Considering the reduction of accidents to be the main purpose for improving the current AWCLS, substantial improvement can be realized using deck heave prediction. Tighter glide path control results in the near elimination of ramp strikes as well as in overall reduction in landing impact velocities. Due to the dominating effect of the severe burble conditions, significant bolter rate improvement was not generally noted with the prediction configuration. However, the decreased standard deviations of landing positions, using prediction, indicate the effect of tighter glide path control. This control could be further exploited through judicious use of both the command and the error ramp inputs to decrease the bolter rate and to increase the probability of landings which meet military specifications. The use of the simulation as an analytical basis for determining error ramp was demonstrated.

B. SEA CONDITION UPPER LIMITS FOR SAFE RECOVERY

For safe aircraft recovery operations using deck heave prediction, the results indicate that for a landing environment similar to that being modeled, upper limits for deck heave and pitch motion correspond to approximate RMS values of 4.949 feet and 0.848 degrees, respectively.

C. THEORETICAL ANALYSIS

The probablistic analysis for the determination of approach and landing dispersions was shown to be a valid technique for comparing competing automatic systems. The implementation of this technique provided a systematic approach for the study of AWCLS performance.

D. GENERALIZATION OF RESULTS

The choice of a single AWCLS/aircraft system for the analysis may restrict the validity of some of the results to that particular system. However, as the most recent concept of the Navy's AWCLS design is as presented in this paper, it is postulated that the results presented are applicable to other aircraft. Correlation of results with other systems should be attempted.

The study was restricted to modification of the existing AWCLS design. Use of pitch and heave prediction to initiate a single terminal maneuver approach instead of improving the AWCLS deck-chase mode should be investigated.

REFERENCES

1. All-Weather Carrier Landing System Airborne Subsystem, General Requirements for, Naval Air Systems Command AR-40, 1 May 1969.

2. Systems Technology, Inc., Report 137-2, Carrier Landing Analyses, by T.S. Durand, February 1967.

3. Naval Air Test Center Report FT-28R-72, Development of the A-7E Airplane Automatic Carrier Landing System (ACLS) Mode I Operational Capability, by LT W. B. Christie, USN and A.P. Shust, Jr., 11 May 1972.

4. Systems Technology, Inc., Report 197-1, An Analysis of Navy Approach Power Compensator Problems and Requirements, by S.J. Craig, R.F. Ringland, and I.L. Ashkenas, March 1971.

5. Systems Technology, Inc., Report 1020-1, Visual Landing Aid Harmonization Analyses, by R.F. Ringland and A.A. Blauvelt, August 1972.

6. Systems Technology, Inc., Technical Proposal No. 251, Proposal for a SPN-42 DMC Lead Computer, May 1972.

7. Etkin, B., Dynamics of Flight, Wiley, 1959.

8. Naval Air Propulsion Test Center Report ATD-211, TF41-A-2 Engine Thrust-Power Level Relationship, by P.F. Piscopo, January 1972.

9. Agnew, H., Naval Air Test Center, Patuxent River, Maryland, Personal Communications to T.M. Judd, 15 February 1973.

10. Wigginton, R.F., Naval Air Test Center, Patuxent River, Maryland, Personal Communications to T.M. Judd, 15 February 1973.

11. Systems Technology, Inc., Report 137-1, An Analysis of Terminal Flight Path Control in Carrier Landings, by T.S. Durand and G.L. Teper, August 1964.

12. North American Aviation, Inc., Columbus Division Report Na66H-289, A Study of Terminal Flight Path Control in Carrier Landings, by R.C. A'Harrah and R.F. Siewert, February 1967.

13. Systems Technology, Inc., Progress Report 15, Contract Nonr-4156(00), Fresnel Lens Optical Landing System, by T.S. Durand, 22 December 1964.

14. IBM Application Program 360A-CX-16X, System/360 Continuous System Modeling Program User's Manual, 4th ed., IBM Corporation, October 1969.

15. Naval Electronics Systems Test and Evaluation Facility, Final Report, Evaluation of Ops-II Operational Program for the Automatic Carrier Landing System, by R.F. Wigginton, 26 February 1971.

TABLE I

AIRCRAFT GEOMETRY AND STABILITY DERIVATIVES

Stability Derivatives		Approach Parameters	
X_u	-0.05435	S	375 ft^2
X_w	0.064327	W	24,000 lb
Z_u	-0.286953	I_{yy}	68,000 slug-ft^2
$Z_{\dot{w}}$	0.0	MAC	10.84 ft
Z_w	-0.528871	m	746 slugs
M_u	-0.000165	h	Sea Level
$M_{\dot{w}}$	-0.000289	ρ	0.002378 $\frac{slugs}{ft^3}$
M_w	-0.007968	U_0	218 ft/s
M_q	-0.327532	α_0	12 deg
X_{δ_e}	0.732836	c.g.	28.6% MAC
Z_{δ_e}	-14.713536	l_x	6.7 ft (ahead of c.g.)
M_{δ_e}	-2.188878	θ_0	8.8 deg (nose up)
$X_{\Delta T}$	0.001317	l_t	13.49 ft (c.g. to c.p. of vertical tail)
$Z_{\Delta T}$	-0.000250	hhc.g.	14.65 ft
$M_{\Delta T}$	0.000004	hvc.g.	4.17 ft

CARRIER GEOMETRY

x_f	233 ft
pcang	16.02 deg
pcran	222 ft
pcalt	64 ft
pcslt	231.04 ft

TABLE II

CONTROL SYSTEMS PARAMETERS

AFCS		APCS	
K_θ	3.6 rad/rad	K_{δ_e}	242.362 volts/rad
$K_{\dot{\theta}}$	1.0 rad/rad-s	T_w	0.1 (nose up); 0.9 (nose down)
K_{n_z}	3.0 deg/g	K_α	2.732 volts/unit α
		K_{α_I}	0.4316 volts/unit α-s
ACLS		T_α	0.95 sec
K_c	0.133	K_{n_z}	27.6 volts/g
K_p	0.56	T_e	f (Thrust)
K_a	0.60		
R_0	1.0 (range<7600 ft)		
t_i	1/15		
t_a	2.85		
t_R	2.0		
K_x	$\frac{6000}{x}(1-0.0625) + 0.0625$		6000 < range < 30,000 ft
	1.0		3000 < range < 6000 ft
	$2.25 - \frac{x}{2400}$		2400 < range < 3000 ft
	1.25		range < 2400 < ft

TABLE III

CSMP FUNCTIONAL BLOCKS

General Form	Function
Y = INTGRL (IC, X) Y(0) = IC Integrator	$Y = \int X\,dt + IC$ Laplace Transform: $\frac{1}{s}$
Y = REALPL (IC, P, X) Y(0) = IC 1st Order Lag	$P\dot{Y} + Y = X$ Laplace Transform: $\frac{1}{Ps + 1}$
Y = DERIV (IC, X) $\dot{X}$ (t=0) = IC Derivative	$Y = \frac{dX}{dt}$ Laplace Transform: s
Y = LEDLAG (P_1, P_2, X) Lead-Lag	$P_2\dot{Y} + Y = P_1\dot{X} + X$ Laplace Transform $\frac{P_1 s + 1}{P_2 s + 1}$
Y = AFGEN (FUNCT, X) Arbitrary Function Generator (Linear Interpolation)	Y = FUNCT(X)
MACRO . . . ENDMAC	These labels are used to identify a group of statements that define a MACRO. This feature allows the user to build larger function blocks from the basic S/360 CSMP and FORTRAN functions.
PROCEDURE . . . ENDPRO	These labels provide a convenient means for using the logic capabilities of FORTRAN in defining new functions. Statements included between the cards labeled PROCEDURE and ENDPRO are not sorted internally but are treated as a single functional entity by the sorting algorithm.

TABLE IV

AIRCRAFT STATE EQUATIONS MATRICES

$$[A]$$

$$\begin{bmatrix} X_u & X_w & -g & 0 \\ \frac{Z_u}{1-Z_{\dot{w}}} & \frac{Z_w}{1-Z_{\dot{w}}} & 0 & U_0 \\ 0 & 0 & 0 & 1.0 \\ M_u+\frac{M_{\dot{w}}Z_u}{1-Z_{\dot{w}}} & M_w+\frac{M_{\dot{w}}Z_w}{1-Z_{\dot{w}}} & 0 & M_q+\frac{M_{\dot{w}}U_0}{1-Z_{\dot{w}}} \end{bmatrix}$$

$$[B]$$

$$\begin{bmatrix} X_{\delta_e} & X_{\Delta T} & -X_u & -X_w \\ Z_{\delta_e} & Z_{\Delta T} & -Z_u & -Z_w \\ 0 & 0 & 0 & 0 \\ M_{\delta_e}+\frac{M_{\dot{w}}Z_{\delta_e}}{1-Z_{\dot{w}}} & M_{\Delta T}+\frac{M_{\dot{w}}Z_{\Delta T}}{1-Z_{\dot{w}}} & -M_u-\frac{M_{\dot{w}}Z_u}{1-Z_{\dot{w}}} & -M_w-\frac{M_{\dot{w}}Z_w}{1-Z_{\dot{w}}} \end{bmatrix}$$

TABLE IV (continued)

[C]

$$\begin{bmatrix} 0 & -1.0 & U_0 & 0 \\ \frac{Z_u}{1-Z_{\dot{w}}} & Z_w & 0 & 0 \\ -1_x\left(M_u + \frac{M_{\dot{w}} Z_u}{1-Z_{\dot{w}}}\right) & -1_x\left(M_w + \frac{M_{\dot{w}} Z_w}{1-Z_{\dot{w}}}\right) & 0 & -1_x\left(M_q + \frac{M_{\dot{w}} U_0}{1-Z_{\dot{w}}}\right) \end{bmatrix}$$

[D]

$$\begin{bmatrix} 0 & 0 & 0 & 0 \\ Z_{\delta_e} & Z_{\Delta T} & -Z_u & -Z_w \\ -1_x\left(M_{\delta_e} + \frac{M_{\dot{w}} Z_{\delta_e}}{1-Z_{\dot{w}}}\right) & -1_x\left(M_{\Delta T} + \frac{M_{\dot{w}} Z_{\Delta T}}{1-Z_{\dot{w}}}\right) & 1_x\left(M_u + \frac{M_{\dot{w}} Z_u}{1-Z_{\dot{w}}}\right) & 1_x\left(M_w + \frac{M_{\dot{w}} Z_w}{1-Z_{\dot{w}}}\right) \end{bmatrix}$$

[E]

$$\begin{bmatrix} 0 & 0 & 0 \\ 0 & 0 & 0 \\ 0 & 1.0 & 0 \end{bmatrix}$$

TABLE V

BASELINE AWCLS CONFIGURATION DATA

Heave: 8 X sin (0.6 X Time + Phase)
Pitch: 1.414 X sin (0.6 X Time + (Phase + 90 deg/57.296))

Updraft-downdraft Burble

Phase	Velocity of Impact	Height of Hook Above Ramp	Landing Position
0.0	24.130	5.528	160.090
10.0	23.980	1.911	182.590
20.0	23.470	-0.690	199.520
30.0	22.930	-3.002	216.440
40.0	22.280	-4.930	233.270
50.0	21.250	-6.430	250.040
60.0	20.030	-7.480	261.250
70.0	18.840	-8.040	272.360
80.0	17.550	-8.080	277.880
90.0	16.210	-7.610	277.850
100.0	14.780	-6.620	266.550
110.0	13.430	-5.139	243.970
120.0	11.880	-3.220	210.080
130.0	9.768	-0.904	147.960
140.0	8.817	1.666	80.030
150.0	9.032	4.626	23.290
160.0	10.200	7.688	-16.550
170.0	11.860	10.750	-39.160
180.0	13.740	13.710	-55.910
190.0	15.730	16.480	-61.260
200.0	17.690	19.030	-60.880
210.0	19.540	21.270	-54.850
220.0	21.250	23.180	-54.590
230.0	22.650	24.680	-49.070
240.0	23.880	25.730	-37.820
250.0	24.850	26.290	-26.550
260.0	25.550	26.350	-15.280
270.0	25.920	25.890	- 3.703
280.0	26.100	24.960	13.360
290.0	26.050	23.570	24.710
300.0	25.870	21.750	41.680
310.0	25.560	19.560	58.640
320.0	25.340	17.080	81.170
330.0	24.940	14.340	98.150
340.0	24.750	11.450	120.630
350.0	24.300	8.484	137.590

TABLE VI

MODIFIED BASELINE CONFIGURATION DATA

Heave: 8 X sin (0.6 X (time + 1.10) + Phase)
Pitch: 1.414 X sin (0.6 X Time + (Phase + 90 deg/57.296))

Updraft-downdraft Burble

Phase	Velocity of Impact	Height of Hook Above Ramp	Landing Position
0.0	19.020	4.004	150.080
10.0	18.310	2.674	161.240
20.0	17.310	1.524	166.830
30.0	16.380	0.595	172.310
40.0	15.520	-0.091	177.750
50.0	14.480	-0.502	177.580
60.0	13.590	-0.606	177.310
70.0	12.660	-0.404	171.390
80.0	11.560	0.099	154.180
90.0	10.870	0.887	136.860
100.0	10.270	1.906	108.270
110.0	10.290	3.041	85.280
120.0	10.810	4.843	62.280
130.0	11.670	6.451	39.560
140.0	12.920	8.094	28.300
150.0	14.350	9.718	22.800
160.0	15.820	11.300	17.420
170.0	17.300	12.810	12.130
180.0	18.760	14.250	12.340
190.0	20.040	15.560	12.290
200.0	21.280	16.690	17.890
210.0	22.360	17.610	23.610
220.0	23.260	18.280	23.670
230.0	23.890	18.690	29.910
240.0	24.350	18.830	35.440
250.0	24.600	18.700	41.330
260.0	24.700	18.300	52.730
270.0	24.560	17.630	58.550
280.0	24.340	16.730	70.010
290.0	23.860	15.590	75.930
300.0	23.390	14.270	87.320
310.0	22.840	12.790	98.780
320.0	22.210	11.180	110.200
330.0	21.530	9.516	121.590
340.0	20.800	7.844	132.980
350.0	20.070	5.491	144.330

TABLE VII

MODIFIED BASELINE CONFIGURATION DATA
WITH ERROR RAMP

Updraft-downdraft Burble

Phase	Velocity of Impact	Height of Hook Above Ramp	Landing Position
0.0	15.890	9.319	89.670
10.0	14.790	7.973	95.270
20.0	13.780	6.823	100.780
30.0	12.600	5.890	100.610
40.0	11.320	5.199	94.790
50.0	10.230	4.791	88.880
60.0	8.960	4.668	71.680
70.0	8.038	4.859	54.370
80.0	7.145	5.342	25.710
90.0	6.553	6.097	-8.625
100.0	6.566	7.083	-37.360
110.0	7.241	8.295	-54.770
120.0	8.531	10.210	-66.710
130.0	10.130	11.810	-66.860
140.0	11.840	13.430	-66.750
150.0	13.420	14.750	-60.540
160.0	15.200	16.370	-60.270
170.0	16.970	17.940	-54.310
180.0	18.570	19.410	-48.530
190.0	20.000	20.720	-42.920
200.0	21.290	21.850	-37.170
210.0	22.410	22.770	-31.530
220.0	23.290	23.460	-25.750
230.0	23.940	23.880	-20.030
240.0	24.310	24.030	- 8.641
250.0	24.420	23.900	- 2.566
260.0	24.310	23.490	3.375
270.0	24.010	22.830	14.890
280.0	23.510	21.910	20.800
290.0	22.900	20.770	32.280
300.0	22.070	19.450	38.190
310.0	21.240	18.000	49.600
320.0	20.200	16.520	55.480
330.0	19.230	14.900	66.870
340.0	18.050	12.490	72.710
350.0	17.070	10.870	83.990

TABLE VIII

MODIFIED AWCLS CONFIGURATION DATA

Heave: 4 X sin (0.6 X (Time + 1.10) + Phase)
Pitch: 0.707 X sin (0.6 X Time + (Phase + 90 deg/57.296))

Updraft-downdraft Burble

Phase	Velocity of Impact	Height of Hook Above Ramp	Landing Position
0.0	16.510	1.842	176.640
10.0	15.580	1.166	171.120
20.0	15.190	0.091	176.640
30.0	15.090	-0.366	187.800
40.0	14.250	-0.704	182.150
50.0	13.730	-0.911	182.040
60.0	13.780	-0.975	193.080
70.0	12.730	-0.885	176.240
80.0	12.290	-0.653	170.470
90.0	12.600	0.030	181.440
100.0	11.630	0.478	153.350
110.0	11.480	1.148	141.920
120.0	11.850	1.948	141.550
130.0	11.600	2.972	113.680
140.0	11.920	3.614	101.940
150.0	12.670	4.427	107.530
160.0	12.900	5.229	85.180
170.0	13.490	5.999	79.680
180.0	14.360	6.731	90.930
190.0	14.750	7.396	74.250
200.0	15.380	7.972	74.280
210.0	16.120	8.434	85.530
220.0	16.410	8.784	74.400
230.0	16.850	8.988	80.100
240.0	17.340	9.062	91.410
250.0	17.400	8.994	85.990
260.0	17.570	8.786	91.410
270.0	17.960	8.443	108.540
280.0	17.660	7.980	103.090
290.0	17.570	7.396	108.820
300.0	17.780	6.721	125.690
310.0	17.360	5.963	125.850
320.0	17.060	5.149	131.610
330.0	17.780	4.300	125.690
340.0	16.560	3.437	148.590
350.0	16.400	2.605	159.890

$$
\begin{bmatrix}
s-X_u & -X_w & g & 0 & 0 & 0 \\
-Z_u & (1-Z_{\dot{w}})s-Z_w & -U_0 s & 0 & 0 & 0 \\
-M_u & -(M_{\dot{w}}s+M_w) & s^2-M_q s & 0 & 0 & 0 \\
0 & 1 & -U_0 & 1 & 0 & 0 \\
0 & -s & U_0 s & 0 & 1 & 0 \\
0 & -s & 1_x s^2+U_0 s & 0 & 0 & 1
\end{bmatrix}
\begin{bmatrix} u \\ w \\ \theta \\ \dot{h} \\ a_z \\ a_z' \end{bmatrix}
=
\begin{bmatrix}
X_{\delta_e} & X_{\Delta T} & -X_u & -X_w \\
Z_{\delta_e} & Z_{\Delta T} & -Z_u & -Z_w \\
M_{\delta_e} & M_{\Delta T} & -M_u & -M_w \\
0 & 0 & 0 & 0 \\
0 & 0 & 0 & 0 \\
0 & 0 & 0 & 0
\end{bmatrix}
\begin{bmatrix} \delta_e \\ \Delta T \\ u_g \\ w_g \end{bmatrix}
$$

FIGURE 1. AIRCRAFT EQUATIONS OF MOTION

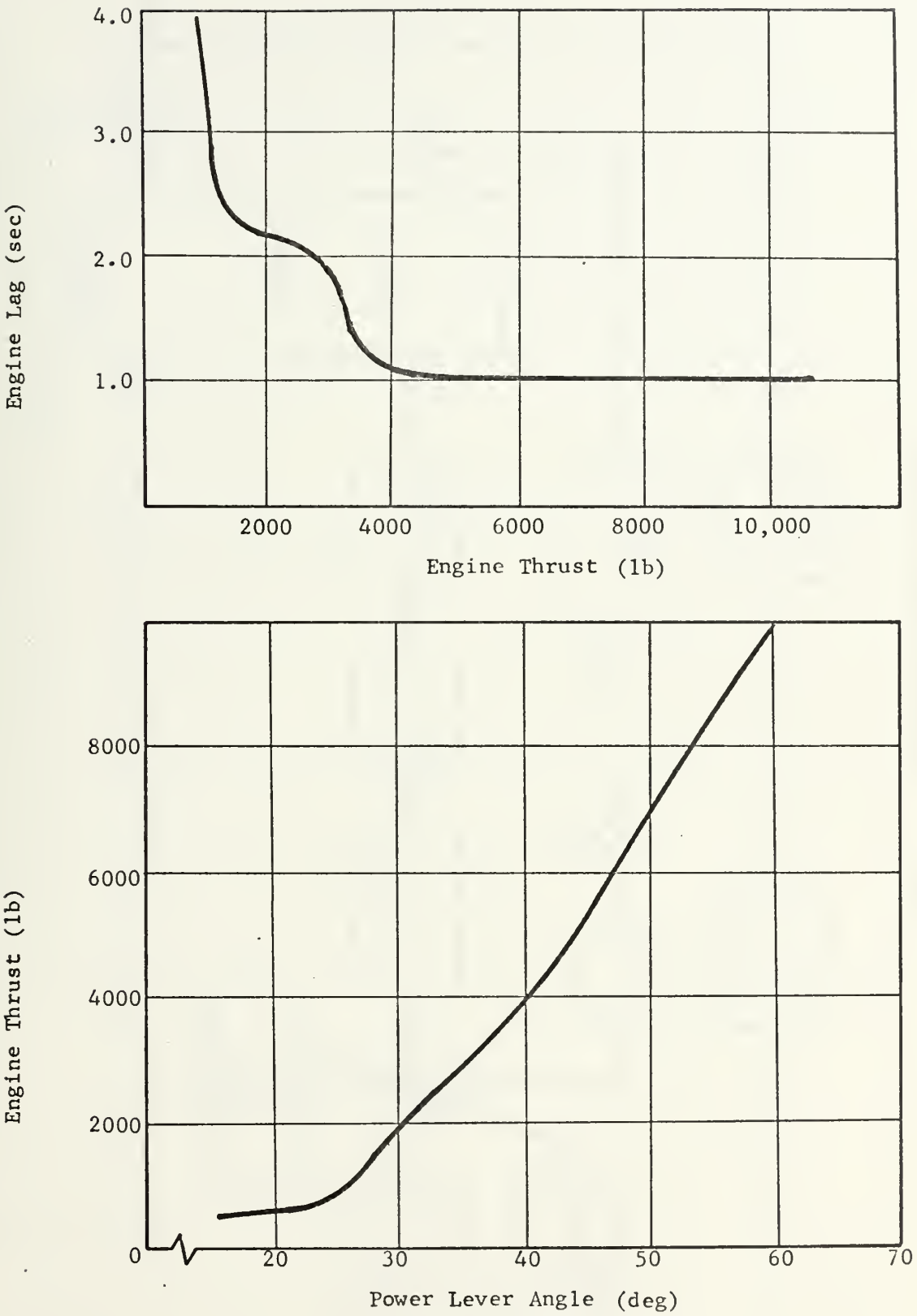

FIGURE 2. TF41-A-2 ENGINE CHARACTERISTICS

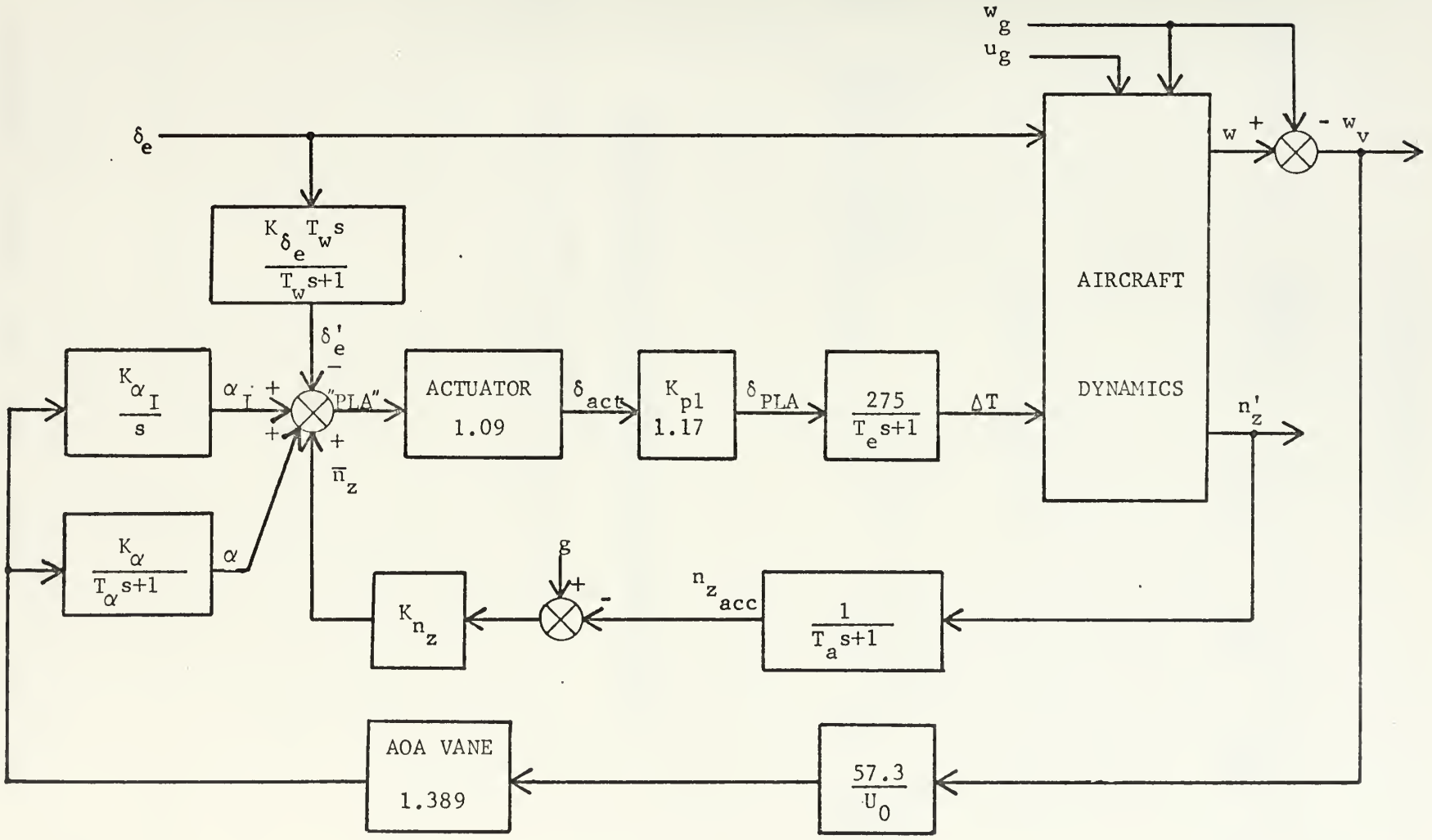

FIGURE 3. STANDARD APCS BLOCK DIAGRAM

AFCS EQUATION

$$\delta_e = \left(K_\theta(\theta-\theta_c) + K_{\dot{\theta}} + \frac{Kn_z N_z}{0.55s+1}\right) \left(\frac{1}{(\frac{s}{20}+1) \quad (\frac{s}{20})^2 + \frac{2(0.7)s}{20} + 1}\right)$$

ACLS EQUATION

$$\frac{\theta_c}{Z_e} = \left(\frac{K_c K_x}{K_p s+1}\right) \left(\frac{\frac{s}{3.9} + 1}{(\frac{s}{5})^2 + \frac{s}{3.5} + 1}\right) \left(\frac{t_i K_x}{s} + 1\right) + \left(\frac{R_0 s}{(\frac{s}{5})^2 + \frac{s}{3.5} + 1}\right)\left(\frac{t_a s}{(K_a s+1)^2} + t_R\right)$$

DECK MOTION COMPENSATION EQUATION

$$\frac{\Delta Z_c}{Z_{11}} = 0.83 \left(\frac{1.11s^2+0.79s+1}{(0.21s+1)^3}\right) \left(\frac{1.5s + 1}{0.5s + 1}\right)$$

FIGURE 4. AFCS, ACLS, DMC TRANSFER FUNCTIONS

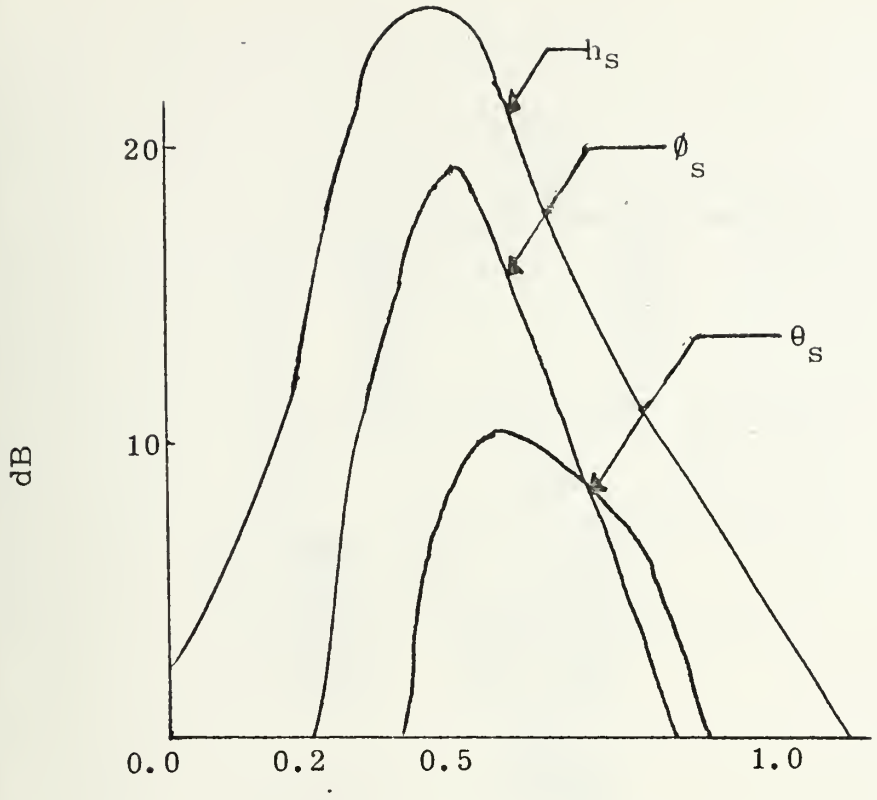

FIGURE 5. SHIP MOTION POWER SPECTRA

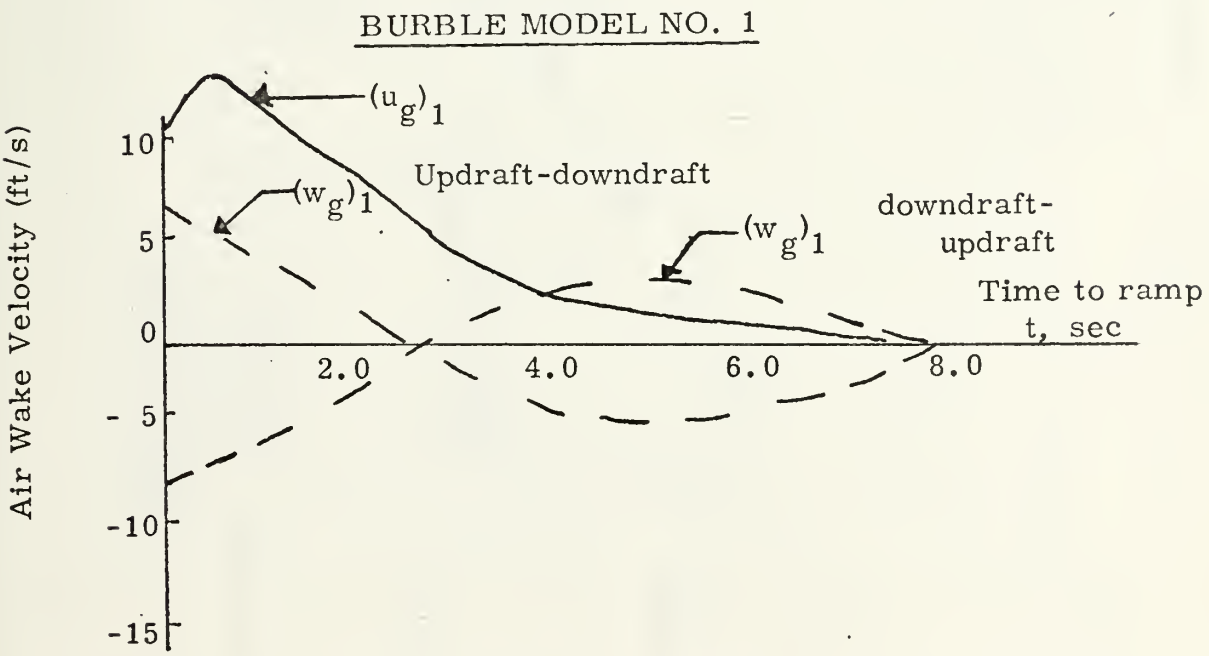

FIGURE 6. SEVERE STEADY-STATE AIR WAKE

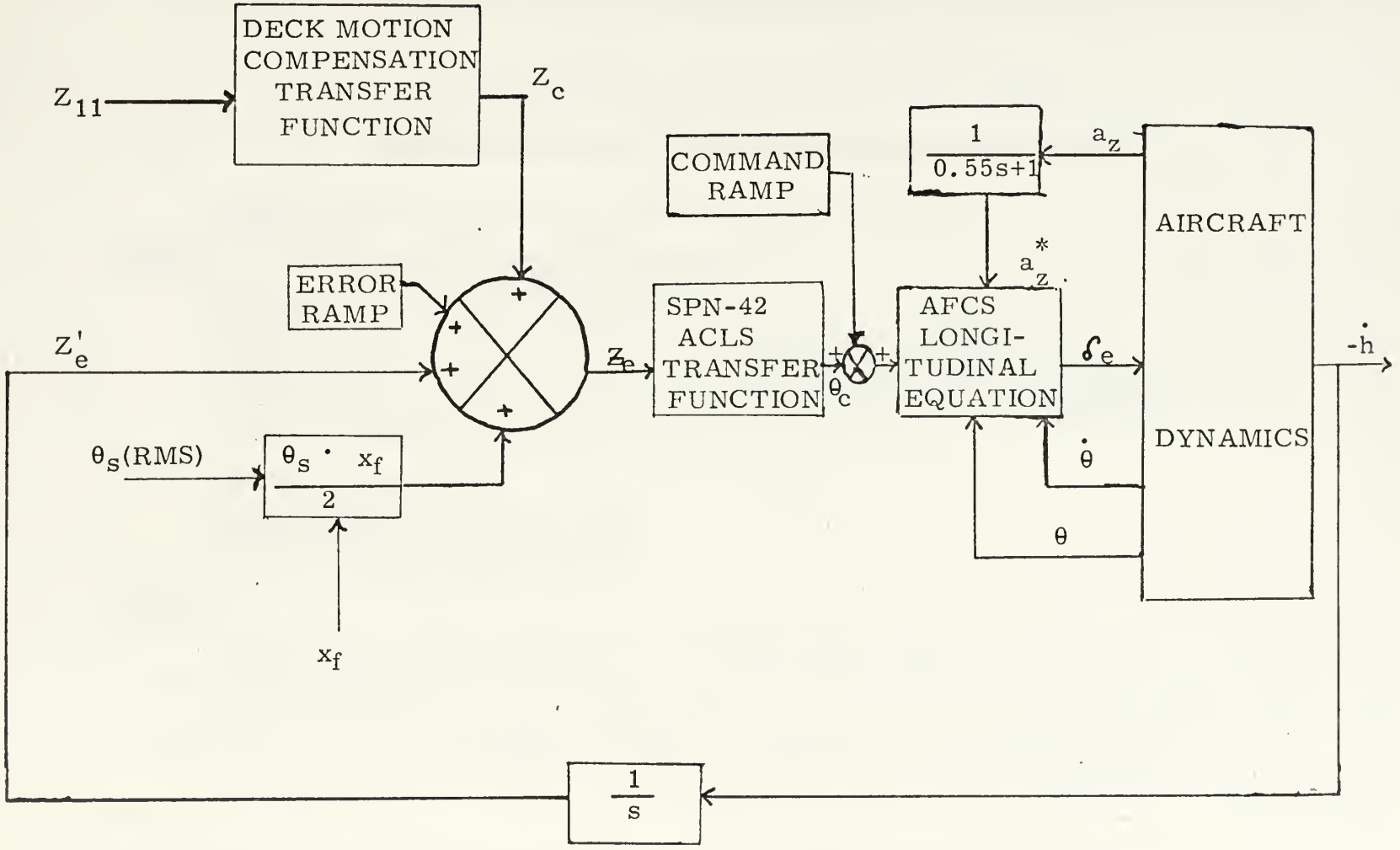

FIGURE 7. STANDARD ACLS BLOCK DIAGRAM

APPENDIX A

CSMP COMPUTER PROGRAM AND SAMPLE OUTPUT

MODIFIED BASELINE CONFIGURATION WITH ERROR RAMP

```
/      DIMENSION A(4,4),B(4,4),C(3,4),D(3,4)
       FIXED I,J
MACRO      DELZC=FUNCT(C0,C1,C2,C6,ZD,D0,D1)
PROCEDURE      ZE=FCN(ZEPRIM,DELZC,PCHXF)
       IF(TIME.LE.15.0)ZE=ZEPRIM+PCHXF
       IF(TIME.GT.15.0.AND.TIME.LE.16.0)ZE=ZEPRIM+PCHXF+1.0
       IF(TIME.GT.16.0.AND.TIME.LE.17.0)ZE=ZEPRIM+PCHXF+2.0
       IF(TIME.GT.17.0.AND.TIME.LE.18.0)ZE=ZEPRIM+PCHXF+3.0
       IF(TIME.GT.18.0.AND.TIME.LE.19.0)ZE=ZEPRIM+PCHXF+4.0+DELZC/2.0
       IF(TIME.GT.19.0.AND.TIME.LE.20.0)ZE=ZEPRIM+PCHXF+5.0+DELZC
       IF(TIME.GT.20.0.AND.TIME.LE.28.5)ZE=ZEPRIM+PCHXF+6.0+DELZC
       IF(TIME.GT.28.5)  ZE=ZE
ENDPRO
       Z1=INTGRL(0.0,Z2)
       Z2=INTGRL(0.0,Z3)
       Z3DOT=ZD-C0*Z1-C1*Z2-C2*Z3
       Z3=INTGRL(0.0,Z3DOT)
       DELZC=(Z3+D1*Z2+D0*Z1)*C6
ENDMAC
INITIAL
NOSORT
       READ(5,100) ((A(I,J),J=1,4),I=1,4),((B(I,J),J=1,4),I=1,4),      ...
       ((C(I,J),J=1,4),I=1,3),((D(I,J),J=1,4),I=1,3)
  100  FORMAT(4F10.6)
       WRITE(6,1000) ((A(I,J),J=1,4),(B(I,J),J=1,4),I=1,4),((C(I,J),   ...
       J=1,4),(D(I,J),J=1,4),I=1,3)
 1000  FORMAT('0',T35,'A-MATRIX',T99,'B-MATRIX'//4(T06,4F15.6,T71,
      $4F15.6/)//T35,'C-MATRIX',T99,'D-MATRIX'//3(T06,4F15.6,T71,
      $4F15.6/)//)
SORT


       FUNCTION AIRWUL=0.0,0.0,18.0,0.0,18.840,+1.5,19.840,+1.5,        ...
       20.84,+1.5,21.840,+1.5,22.840,+2.0,23.840,+3.0,24.840,+4.25,    ...
       25.840,+6.3,26.840,+9.5,27.840,+13.75,28.840,+8.75,28.85,0.0,   ...
       30.0,0.0,33.0,0.0
```

```
      FUNCTION AIRWU2=0.0,0.0,18.0,0.0,18.880,+1.5,19.880,+1.5,        ...
      20.88,+1.5,21.880,+1.5,22.880,+2.0,23.880,+3.0,24.880,+4.25,    ...
      25.880,+6.3,26.880,+9.5,27.880,+13.75,28.880,+8.75,28.89,0.0,   ...
      30.0,0.0,33.0,0.0


      FUNCTION AIRWUD=0.0,0.0,18.0,0.0,18.840,0.0,19.840,0.0,20.840, ...
      0.0,21.840,-2.5,22.840,-3.7,23.840,-4.0,24.840,-3.0,25.840,     ...
      -0.75,26.840,2.0,27.840,5.0,28.840,7.0,28.85,0.0,30.0,0.0,33.0,0.0


      FUNCTION AIRWDU=0.0,0.0,18.0,0.0,18.880,0.0,19.880,0.0,20.880, ...
      0.0,21.880,+2.5,22.880,+3.7,23.880,+4.0,24.880,+3.0,25.880,     ...
      +0.75,26.880,-2.,27.880,-5.,28.880,-7.,28.89,0.0,30.0,0.0,33.0,0.0


      FUNCTION TECURV=-2100.0,4.0,-1800.0,2.5,-1500.0,2.25,-1200.0,   ...
      2.18,-800.0,2.13,-400.0,2.08,-200.0,2.03,0.0,1.85,200.0,1.55,   ...
      400.0,1.27,600.0,1.15,800.0,1.1,1200.0,1.05,2000.0,1.0,3000.0,  ...
      1.0
      PARAM AMPP=1.0,FRP=0.60,AMH =8.0,FRH=0.60,C0=107.9797,C6=99.4817
      PARAM C2=14.2857,C1=68.0272,D0=0.9009,D1=0.7117,R0=1.0,B6=3.168
      PARAM A0=25.0,A1=253.685,A2=195.2946,A3=70.2927,A4=12.2619
      PARAM TI=0.0667,TR=2.0,TA=2.85,KC=0.133,KP=0.56,KA=0.6
      PARAM XF=233.0,V0=218.0,THETA0=0.15358
      PARAM PCANG=.28068,PCRAN=222.0,PCALT=64.0,PCSLT=231.04
      PARAM   PHASE= 0.0
      INCON X10=0.0,X20=0.0,X30=0.0,X40=0.0,ZE0=0.0
      INCON TD=0.0,RT=0.0,RAMPR=0.0,RALT=0.0,HTMG=0.0,TDRANG=0.0
PROCEDURE       BETA=FUNC(AMPP)
      IF(AMPP.LT.0.501) BETA=.06108
      IF(AMPP.GE.0.501.AND.AMPP.LT.0.6) BETA=.06981
      IF(AMPP.GE.0.6.AND.AMPP.LT.0.7) BETA=.07155
      IF(AMPP.GE.0.7.AND.AMPP.LT.0.8) BETA=.0733
      IF(AMPP.GE.0.8.AND.AMPP.LT.0.9) BETA=.07504
      IF(AMPP.GE.0.9.AND.AMPP.LT.1.0) BETA=.07679
      IF(AMPP.GE.1.0) BETA=.07853
ENDPRO
PROCEDURE     ALT0,RANG0=FNC(V0,BETA)
      RANG0=30.0*V0*COS(BETA)+(3.67+2.0*SIN(THETA0))*TAN(BETA)
      ALT0=30.0*V0*SIN(BETA)+(3.67+2.0*SIN(THETA0))
ENDPRO
DYNAMIC
*
*
*     AIRCRAFT EQUATIONS OF MOTION
*
      UGUST=AFGEN(AIRWU1,TIME)
```

```
      WGUST=AFGEN(AIRWUD,TIME)
      XTEMP1=A(1,1)*X1+A(1,2)*X2+A(1,3)*X3+A(1,4)*X4+B(1,1)*ELEV      ...
      +B(1,2)*THRUST+B(1,3)*UGUST+B(1,4)*WGUST
      X1=INTGRL(X10,XTEMP1)
      XTEMP2=A(2,1)*X1+A(2,2)*X2+A(2,3)*X3+A(2,4)*X4+B(2,1)*ELEV      ...
      +B(2,2)*THRUST+B(2,3)*UGUST+B(2,4)*WGUST
      X2=INTGRL(X20,XTEMP2)
      X3=INTGRL(X30,X4)
      XTEMP4=A(4,1)*X1+A(4,2)*X2+A(4,3)*X3+A(4,4)*X4+B(4,1)*ELEV      ...
      +B(4,2)*THRUST+B(4,3)*UGUST+B(4,4)*WGUST
      X4=INTGRL(X40,XTEMP4)
      HDOT  =C(1,1)*X1+C(1,2)*X2+C(1,3)*X3+C(1,4)*X4
      AZ    =C(2,1)*X1+C(2,2)*X2+C(2,3)*X3+C(2,4)*X4+D(2,1)*ELEV      ...
      +D(2,2)*THRUST+D(2,3)*UGUST+D(2,4)*WGUST
      AZPRIM=C(3,1)*X1+C(3,2)*X2+C(3,3)*X3+C(3,4)*X4+D(3,1)*ELEV      ...
      +D(3,2)*THRUST+D(3,3)*UGUST+D(3,4)*WGUST+AZ
*
**      SHIP PITCHING MOTION - LEADS HEAVE BY NINETY DEGREES
*
      PITCH=((AMPP)/57.296)*SIN(FRP*TIME+(PHASE+90.0)/57.296)
      PTICH=PITCH/0.707
      ZC2=PCSLT*PTICH*COS(PCANG)
      PCHXF=AMPP*XF*0.5/57.296
      PTCH=ABS(PTICH)
*
**    A-7E SPN-42 TRANSFER FUNCTION EQUATIONS
*
      Z12=AMH*SIN(FRH*TIME+PHASE/57.296)
      Z11=AMH*SIN(FRH*(TIME+1.10)+PHASE/57.296)
      ZD=LEDLAG(1.5,0.5,Z11)
      ZEPRIM=INTGRL(ZE0,-HDOT)
      DELZC=FUNCT(C0,C1,C2,C6,ZD,D0,D1)
      ZE=FCN(ZEPRIM,DELZC,PCHXF)
      XDOT=(V0+X1)*COS(BETA)  +V0*X3*SIN(BETA)  -X2*SIN(BETA)
      ZDOT=(V0+X1)*SIN(BETA)-(V0*X3)*COS(BETA)+X2*COS(BETA)
      RAN=INTGRL(0.0,XDOT)
      RANG=RANG0-RAN
PROCEDURE       K=FNT(RANG)
      KX=(6000.0/RANG)*(1.0-0.0625)+0.0625
      KY=1.00
      KZ=2.25-(RANG/2400.0)
      IF(RANG.GE.6000.0) K=KX
      IF(RANG.LT.6000.0.AND.RANG.GE.3000.0) K=KY
      IF(RANG.LT.3000.0.AND.RANG.GE.2400.0) K=KZ
      IF(RANG.LT.2400.0) K=1.25
ENDPRO
      B3=((KA**2.0)*(TI*K+3.9)+(2.0*KA)*(3.9*R0*TR+1.0)+3.9*R0*TA)/B6
      B2=((KA**2.0)*(3.9*TI*K)+(2.0*KA)*(TI*K+3.9)+(3.9*R0*TR+1.0))/B6
```

```
      B1=((2.0*KA)*(3.9*TI*K)+(TI*K+3.9))/B6
      B0=(3.9*TI*K)/B6
      K0=(25.0/3.9)*KC*(K/KP)*(3.9*R0*TR+1.0)*(1.0/57.296)
      ZI=K0*INTGRL(0.0,ZE)
      Y0=INTGRL(0.0,Y1)
      Y1=INTGRL(0.0,Y2)
      Y2=INTGRL(0.0,Y3)
      Y3=INTGRL(0.0,Y4)
      Y4DOT=ZI-A4*Y4-A3*Y3-A2*Y2-A1*Y1-A0*Y0
      Y4=INTGRL(0.0,Y4DOT)
      THETAC=Y4+B3*Y3+B2*Y2+B1*Y1+B0*Y0
*
*     A-7E LONGITUDINAL AFCS EQUATION
*
      AZSTAR=REALPL(0.0,0.55,AZ)
      ELEV=3.6*(X3-THETAC)+X4-0.00163*AZSTAR
*
*     A-7E APC LOOP CLOSURES
*
      ALPHAV=0.3651*(X2-WGUST)
      ALPHAI=0.4316*INTGRL(0.0,ALPHAV)
      ALPHA=INTGRL(0.0,(2.732*ALPHAV-ALPHA)/0.95)
PROCEDURE       TW=FCTN(ELEV)
      IF(ELEV.GT.0.0) TW=0.9
      IF(ELEV.LE.0.0) TW=0.1
ENDPRO
      W1DOT=-(1.0/TW)*W1+ELEV
      W1=INTGRL(0.0,W1DOT)
      ELEVP=242.362*W1DOT
      NZP=1.0-0.03109*AZPRIM
      NZACC=REALPL(1.0,1.0,NZP)
      NZBAR=27.6*(1.0-NZACC)
      PLA=NZBAR+ALPHA+ALPHAI-ELEVP
      TE=AFGEN(TECURV,THRUST)
      THRUST=INTGRL(0.0,(350.7*PLA-THRUST)/TE)
*
*     A-7E CARRIER APPROACH PROFILE
*
      AL=INTGRL(0.0,ZDOT)
      ALT=ALT0-AL
      HCGHK=4.17+14.65*SIN(THETA0+X3)
      CAB=PCRAN+PCALT*SIN(PTICH)
      CABSQ=CAB**2
      BCA=PCSLT*PTCH
      BCASQ=BCA**2
PROCEDURE     DECANG=FUNC(PTICH,PCANG)
      IF(PTICH.GE.0.0)DECANG=(90.0/57.296)-PCANG-PTICH
      IF(PTICH.LT.0.0)DECANG=(90.0/57.296)+PCANG
```

```
ENDPRO
      ABC=SQRT(CABSQ+BCASQ-2.0*BCA*CAB*COS(DECANG))
      ABCSQ=ABC**2
      BCAN=ATAN((2.0*BCA*SIN(DECANG)*CAB)/(ABCSQ+CABSQ-BCASQ))
PROCEDURE BCANG=FUN(BCAN,PTICH)
      IF(PTICH.GE.0.0) BCANG=BCAN
      IF(PTICH.LT.0.0) BCANG=-BCAN
ENDPRO
      HTMGTD=ALT-(RANG+CAB)*TAN(BCANG)-Z12-3.67-2.0*SIN(THETA0+X3)
      SINKR=SQRT((XDOT**2)+(ZDOT**2))*SIN(-BCANG+ATAN(ZDOT/XDOT))
      ZC4=Z12+ZC2
      VTD=DERIV(0.0,ZC4)
      VIMP=SINKR+VTD
      ZC5=ABS(HTMGTD)
      RAMP=ABS((RANG+CAB)-(PCRAN+XF)*COS(BCANG))
PROCEDURE   RT,RAMPR,RALT=FCN(RAMP)
      IF(RAMP.LE.6.0) RT=TIME
      IF(RAMP.LE.6.0) RALT=ALT-(RANG+CAB)*TAN(BCANG)-HCGHK-Z12
      IF(RAMP.LE.6.0) RAMPR=RANG
ENDPRO
PROCEDURE    HTMG,TD,TDRANG,VIMPAC =FCTN(ZC5,RANG,VIMP)
      IF(ZC5.LE.1.0) VIMPAC =VIMP
      IF(ZC5.LE.1.0) TDRANG=RANG
      IF(ZC5.LE.1.0) HTMG=ZC5
      IF(ZC5.LE.1.0) TD=TIME
ENDPRO
*
      TIMER FINTIM=33.0,DELT=0.0500
      METHOD RKSFX
      PREPARE ALT,Z11
TERMINAL
      WRITE(6,1998) VIMPAC
 1998 FORMAT('0','VELOCITY OF IMPACT AT TOUCHDOWN IS',F14.6)
      WRITE(6,1999)
 1999 FORMAT('0',T3,'RAMP TIME',T15,'RAMP RANGE',T30,'RAMP ALT',
     $T45,'TD TIME',T56,'HT MAIN GEAR',T72,'TD RANGE')
      WRITE(6,2001) RT,RAMPR,RALT,TD,HTMG,TDRANG
 2001 FORMAT('0',6F14.4)
      BETA=BETA*57.296
      WRITE(6,2000) BETA
 2000 FORMAT('0',T10,'GLIDESLOPE ANGLE IS',F10.2)
END
```

```
DATA
-0.05453   0.06433    -32.16      0.0
-0.2870    -0.5289    0.0         218.0
0.0        0.0        0.0         1.0
-0.000082  -0.007811  0.0         -0.3905
0.7328     0.001317   0.05453     -0.06433
-14.714    -0.00025   0.28695     0.52887
0.0        0.0        0.0         0.0
-2.1846    0.000004   0.000082    0.007811
0.0        -1.0       218.0       0.0
-0.28695   -0.52887   0.0         0.0
0.00055    0.052334   0.0         2.61635
0.0        0.0        0.0         0.0
-14.714    -0.00025   0.28695     0.52887
14.6368    -0.000027  -0.00055    -0.052334
ENDDATA
STOP
ENDJCB
```

```
                    *** CSMP/360 SIMULATION DATA ***
      FUNCTION AIRWU1=0.0,0.0,18.0,0.0,18.840,+1.5,19.840,+1.5,        ...
      20.84,+1.5,21.840,+1.5,22.840,+2.0,23.840,+3.0,24.840,+4.25,    ...
      25.840,+6.3,26.840,+9.5,27.840,+13.75,28.840,+8.75,28.85,0.0,   ...
      30.0,0.0,33.0,0.0
      FUNCTION AIRWU2=0.0,0.0,18.0,0.0,18.880,+1.5,19.880,+1.5,        ...
      20.88,+1.5,21.880,+1.5,22.880,+2.0,23.880,+3.0,24.880,+4.25,    ...
      25.880,+6.3,26.880,+9.5,27.880,+13.75,28.880,+8.75,28.89,0.0,   ...
      30.0,0.0,33.0,0.0
      FUNCTION AIRWUD=0.0,0.0,18.0,0.0,18.840,0.0,19.840,0.0,20.840,  ...
      0.0,21.840,-2.5,22.840,-3.7,23.840,-4.0,24.840,-3.0,25.840,     ...
      -0.75,26.840,2.0,27.840,5.0,28.840,7.0,28.85,0.0,30.0,0.0,33.0,0.0
      FUNCTION AIRWDU=0.0,0.0,18.0,0.0,18.880,0.0,19.880,0.0,20.880,  ...
      0.0,21.880,+2.5,22.880,+3.7,23.880,+4.0,24.880,+3.0,25.880,     ...
      +0.75,26.880,-2.,27.880,-5.,28.880,-7.,28.89,0.0,30.0,0.0,33.0,0.0
      FUNCTION TECURV=-2100.0,4.0,-1800.0,2.5,-1500.0,2.25,-1200.0,   ...
      2.18,-800.0,2.13,-400.0,2.08,-200.0,2.03,0.0,1.85,200.0,1.55,   ...
      400.0,1.27,600.0,1.15,800.0,1.1,1200.0,1.05,2000.0,1.0,3000.0,  ...
      1.0
      PARAM AMPP=1.0,FRP=0.60,AMP=8.0,FRH=0.60,C0=107.9797,C6=99.4817
      PARAM C2=14.2857,C1=68.0272,D0=0.9009,D1=0.7117,R0=1.0,B6=3.168
      PARAM A0=25.0,A1=253.685,A2=195.2946,A3=70.2927,A4=12.2619
      PARAM TI=0.0667,TR=2.0,TA=2.85,KC=0.133,KP=0.56,KA=0.6
      PARAM XF=233.0,V0=218.0,THETA0=0.15358
      PARAM PCANG=.28068,PCRAN=222.0,PCALT=64.0,PCSLT=231.04
      PARAM   PHASE=90.0
      INCON X10=0.0,X20=0.0,X30=0.0,X40=0.0,ZE0=0.0
      INCON TD=0.0,RT=0.0,RAMPR=0.0,RALT=0.0,HTMG=0.0,TDRANG=0.0
      TIMER FINTIM=33.0,DELT=0.0500,PRDEL=1.0
      METHOD RKSFX
      PRINT ALT,RANG,X3,THETAC,ZE,THRUST,ELEV,ALPHA
END

TIMER VARIABLES
 DELT   = 5.0000E-02
 DELMIN= 3.3000E-06
 FINTIM= 3.3000E 01
 PRDEL  = 1.0000E 00
 OUTDEL= 0.0
```

CSMP RKSFX INTEGRATION

TIME	ALT	RANG	X3	THETAC	ZE	THRUST	ELEV	ALPHA
0.0	5.1703E 02	6.5202E 03	0.0	0.0	2.0333E 00	0.0	0.0	0.0
1.0000E 00	4.9995E 02	6.3028E 03	1.5246E-02	1.6210E-02	2.0111E 00	-2.2422E 01	1.4380E-02	9.1313E-01
2.0000E 00	4.8399E 02	6.0857E 03	6.3856E-03	2.8618E-03	8.9153E-01	2.8451E 02	-3.7280E-03	1.3559E 00
3.0000E 00	4.6812E 02	5.8685E 03	-2.1975E-03	-4.4665E-03	-3.2628E-01	2.2214E 02	4.2856E-03	-2.6347E-01
4.0000E 00	4.5161E 02	5.6511E 03	-2.9021E-03	-3.3337E-03	-9.2597E-01	5.5875E 01	2.3481E-03	-8.8023E-01
5.0000E 00	4.3467E 02	5.4336E 03	-1.6457E-03	-2.3145E-03	-1.0979E 00	-4.8261E 01	2.2307E-03	-6.9138E-01
6.0000E 00	4.1755E 02	5.2162E 03	-1.8893E-03	-2.3532E-03	-1.0823E 00	-5.9530E 01	9.9583E-04	-4.6897E-01
7.0000E 00	4.0028E 02	4.9988E 03	-2.0588E-03	-2.2094E-03	-9.2070E-01	-5.6770E 01	4.2182E-04	-3.3870E-01
8.0000E 00	3.8291E 02	4.7815E 03	-1.7316E-03	-1.6193E-03	-6.4840E-01	-4.3552E 01	-3.7291E-05	-2.0577E-01
9.0000E 00	3.6549E 02	4.5642E 03	-1.1591E-03	-8.8530E-04	-3.3191E-01	-4.5806E 01	-4.1129E-04	-6.4483E-02
1.0000E 01	3.4809E 02	4.3469E 03	-5.7422E-04	-2.0350E-04	-3.2247E-02	-3.8921E 01	-7.0496E-04	5.4572E-02
1.1000E 01	3.3074E 02	4.1296E 03	-1.9244E-05	3.8709E-04	2.1203E-01	-2.2914E 01	-8.2629E-04	1.3902E-01
1.2000E 01	3.1348E 02	3.9123E 03	4.5541E-04	8.2720E-04	3.7701E-01	-3.5602E 00	-7.9153E-04	1.8880E-01
1.3000E 01	2.9631E 02	3.6950E 03	7.7636E-04	1.0560E-03	4.5163E-01	1.4760E 01	-6.3299E-04	2.0245E-01
1.4000E 01	2.7922E 02	3.4777E 03	9.0596E-04	1.0595E-03	4.3923E-01	2.8519E 01	-3.8924E-04	1.8100E-01
1.5000E 01	2.6220E 02	3.2604E 03	8.5057E-04	8.7000E-04	3.5610E-01	3.5379E 01	-1.1015E-04	1.3151E-01
1.6000E 01	2.4524E 02	3.0431E 03	8.5139E-03	8.7994E-03	1.2169E 00	2.5650E 01	8.0169E-03	5.3412E-01
1.7000E 01	2.2888E 02	2.8258E 03	1.2548E-02	1.2587E-02	1.4810E 00	1.5331E 02	4.0006E-03	1.1940E 00
1.8000E 01	2.1326E 02	2.6084E 03	1.3141E-02	1.0110E-02	1.0053E 00	2.3569E 02	9.6456E-03	1.2448E 00
1.9000E 01	1.9810E 02	2.3910E 03	3.9849E-02	3.9999E-02	3.1737E 00	2.6926E 02	3.5334E-02	2.4617E 00
2.0000E 01	1.8505E 02	2.1735E 03	3.8470E-02	1.4731E-02	1.3423E 00	4.3707E 02	5.6189E-02	4.1374E 00
2.1000E 01	1.7301E 02	1.9562E 03	-2.6765E-02	-5.2088E-02	-6.1166E 00	2.2765E 02	2.5505E-02	-1.4323E 00
2.2000E 01	1.5674E 02	1.7387E 03	-6.3952E-02	-7.0359E-02	-1.0699E 01	-3.0973E 00	7.4367E-03	-7.0740E 00
2.3000E 01	1.3571E 02	1.5201E 03	-5.0310E-02	-4.4301E-02	-9.6175E 00	-1.8095E 02	-1.0227E-03	-5.9041E 00
2.4000E 01	1.1325E 02	1.3006E 03	-2.4769E-02	-1.4398E-02	-5.2626E 00	-3.9491E 02	-1.3968E-02	-1.1659E 00
2.5000E 01	9.1938E 01	1.0804E 03	-3.1788E-03	9.5488E-03	1.3092E-01	-2.0129E 02	-2.2423E-02	2.4813E 00
2.6000E 01	7.2451E 01	8.5980E 02	1.8568E-02	3.2003E-02	5.4034E 00	2.8951E 02	-2.3219E-02	4.3304E 00
2.7000E 01	5.4655E 01	6.3874E 02	3.9835E-02	5.1216E-02	9.5797E 00	1.0335E 03	-1.9302E-02	5.2650E 00
2.8000E 01	3.8065E 01	4.1681E 02	5.5001E-02	6.1995E-02	1.1794E 01	1.7145E 03	-1.3064E-02	5.4801E 00
2.9000E 01	2.2490E 01	1.9361E 02	5.9882E-02	6.3369E-02	1.1947E 01	2.1574E 03	-1.3670E-02	5.7484E 00
3.0000E 01	1.1352E 01	-3.1176E 01	6.1175E-02	7.5399E-02	1.1947E 01	2.3474E 03	-2.5774E-02	5.7007E 00
3.1000E 01	5.0166E 00	-2.5723E 02	8.1101E-02	9.0545E-02	1.1947E 01	2.0397E 03	-9.5647E-03	4.6606E 00
3.2000E 01	3.3008E 00	-4.8358E 02	9.6216E-02	1.0531E-01	1.1947E 01	1.9317E 03	-1.0366E-02	3.7077E 00
3.3000E 01	5.6475E 00	-7.0946E 02	1.1182E-01	1.2004E-01	1.1947E 01	1.8514E 03	-8.0605E-03	2.9753E 00

VELOCITY OF IMPACT AT TOUCHDOWN IS 6.554016

RAMP TIME	RAMP RANGE	RAMP ALT	TD TIME	HT MAIN GEAR	TD RANGE
28.8500	227.1797	6.0962	29.9000	0.9201	-8.6250

GLIDESLOPE ANGLE IS 4.50

```
C      OFFLINE PLOTTING ROUTINE
C
C
       DIMENSION XOUT(5),X(900),Y(900),Z(900)
       REAL * 8 LABEL/8H        /,ITITLE(12)
       DATA ENDS/'ENDS'/
       DOUBLE PRECISION WORD
C      KGRAPH IS NO OF OUTPUT VARIABLES
       KGRAPH=3
C      READ CONSTANTS FOR DRAW
       READ(5,100) NOPLOT
     5 READ(5,100) NOCUR
   100 FORMAT(I2)
       READ(5,200) (ITITLE(I),I=1,12)
   200 FORMAT(6A8)
       READ(5,300) XSCL,YSCL,IUP,IRITE,MODEX,MODEY,IW,IHI,IGR
   300 FORMAT(9I5)
       IF(NOCUR-1) 55,10,15
    10 MODCUR=0
       GO TO 20
    15 MODCUR=1
C      READ DATA SET OF POINTS PRODUCED BY CSMP
    20 CONTINUE
C      READ 10 INTRODUCTORY RECORDS
       DO 25 I=1,10
    25 READ (15) WORD
       NUMPTS=0
C      READ POINTS
    30 READ (15) (XOUT(I),I=1,KGRAPH)
       IF(XOUT(1)-ENDS) 35,40,35
    35 NUMPTS=NUMPTS+1
       X(NUMPTS)=XOUT(1)
       Y(NUMPTS)=XOUT(2)
       Z(NUMPTS)=XOUT(3)
       GO TO 30
    40 CONTINUE
C      CALL DRAW
       CALL DRAW(NUMPTS,X,Y,MODCUR,0,LABEL,ITITLE,XSCL,YSCL,IUP,IRITE,
      CMODEX,MODEY,IW,IHI,IGR,LAST)
       READ(5,200) (ITITLE(I),I=1,12)
       CALL DRAW(NUMPTS,X,Z,MODCUR,0,LABEL,ITITLE,XSCL,YSCL,IUP,IRITE,
      CMODEX,MODEY,IW,IHI,IGR,LAST)
       NOCUR=NOCUR-1
```

```
      IF(NOCUR-1) 55,45,50
   45 MCDCUR=3
      READ (15) WORD
      GO TO 20
   50 MCDCUR=2
      READ (15) WORD
      GO TO 20
   55 NOPLOT=NOPLOT-1
      IF(NOPLCT) 60,60,5
   60 STOP
      END
C
C     DATA CARDS

 1
 1
A-7E AIRCRAFT CARRIER APPROACH PROFILE
ALTITUDE RESPONSE VS TIME  JUDD
    C     0     0     0     0     0     8     4     1
A-7E AIRCRAFT APPROACH CARRIER PROFILE
HEAVE INPUT VS TIME    JUDD
```

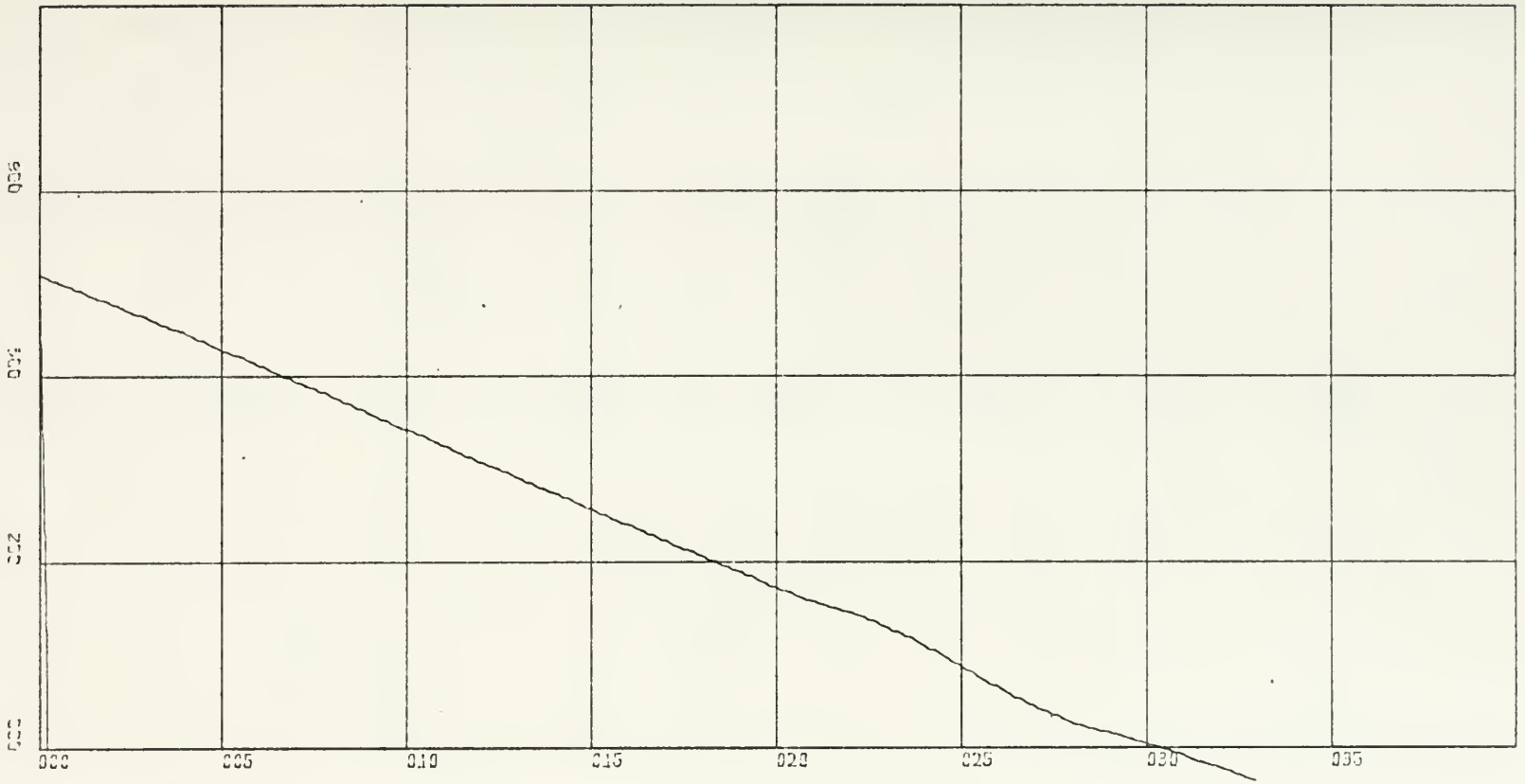

X-SCALE=5.00E+00 UNITS INCH.
Y-SCALE=2.00E+02 UNITS INCH.

A-7E AIRCRAFT CARRIER APPROACH PROFILE
ALTITUDE RESPONSE VS TIME JUDD

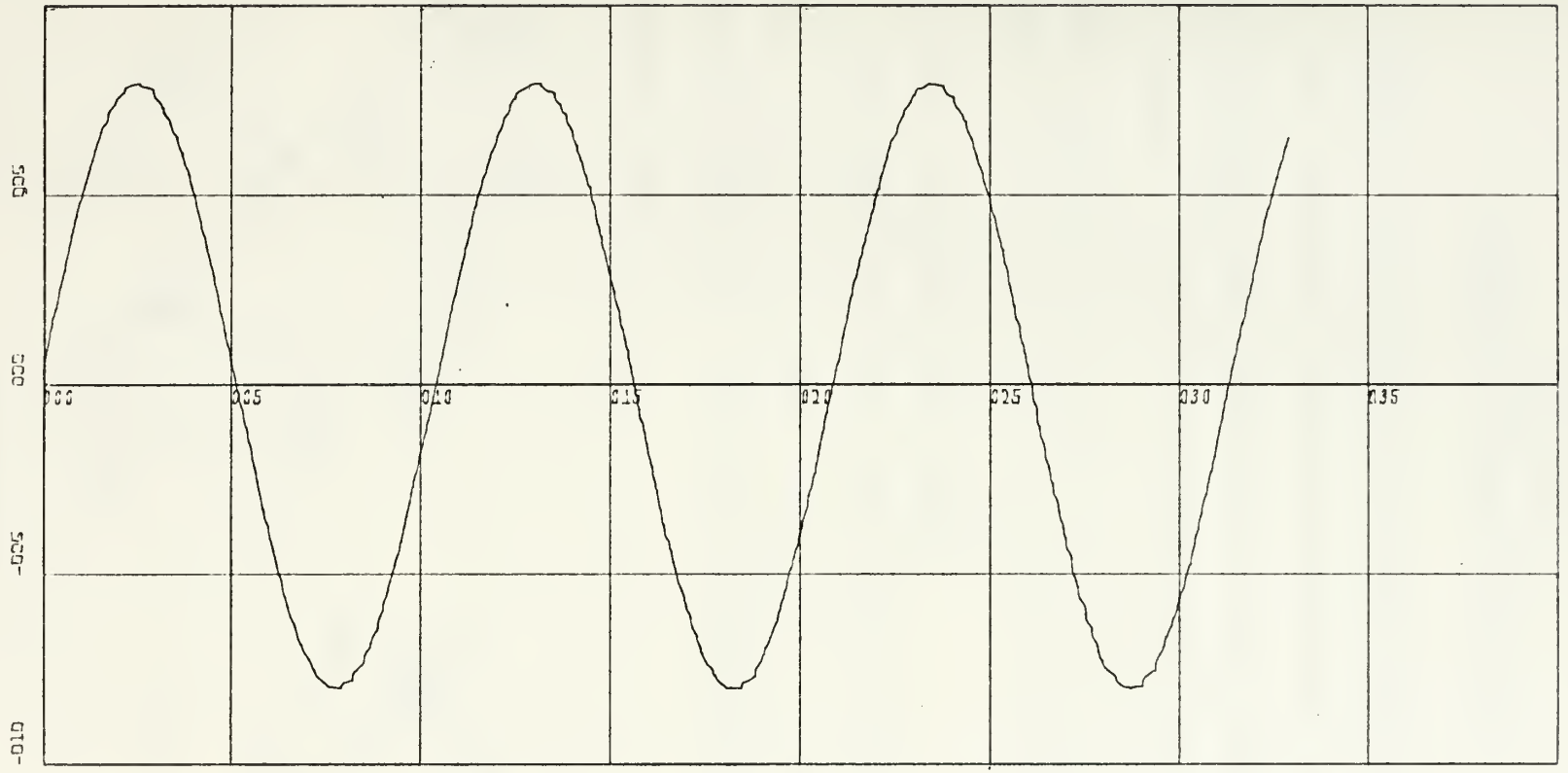

K-SCALE=5.00E+00 UNITS INCH.
Y-SCALE=5.00E+00 UNITS INCH.
A-7E AIRCRAFT APPROACH CARRIER PROFILE
HEAVE INPUT VS TIME JUDD

APPENDIX B

CARRIER APPROACH ANALYSIS

Carrier ramp-crossing time, height of aircraft hook above ramp, time and position of main gear touchdown, and velocity of impact were determined using carrier and aircraft geometry, and known approach parameters. Aircraft altitude and range were always referenced to the position of the ideal touchdown point. The location of carrier pitch center at a point 64 feet below the carrier flight deck led to the following analysis.

For positive and negative pitch of the carrier, positive defined here as ramp up, some means was needed to measure the resulting pitch of the flight deck. The manner in which this was accomplished is shown in Figure B.1.

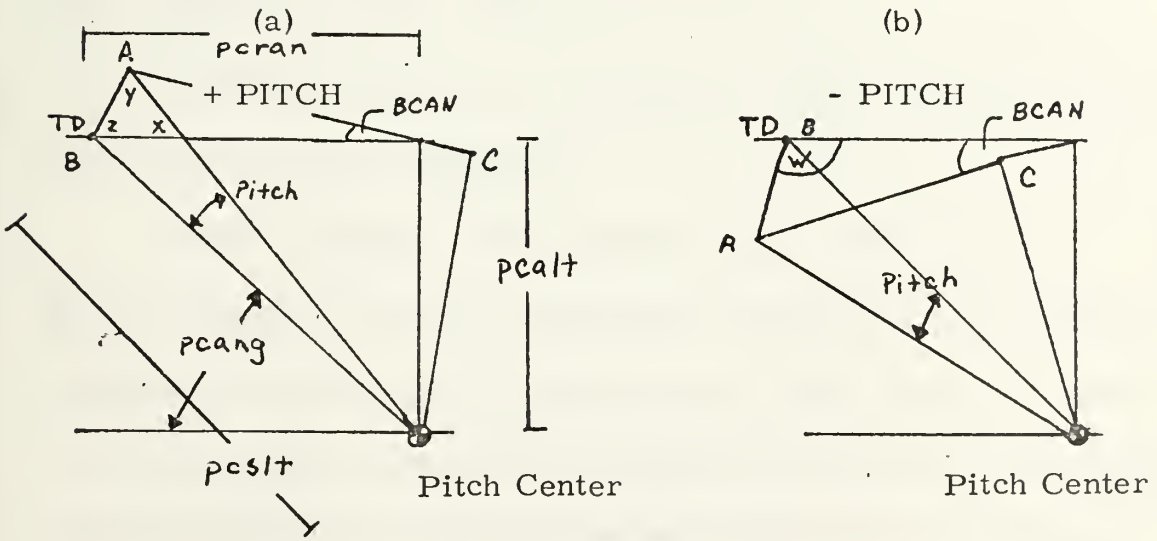

FIGURE B.1.

The angle to be measured is approximately the angle named in Fig. B.1.(a) as BCAN. This is obtained by finding sides BC and BA of triangle BAC. Angle 'x' equals the sum of 'pcang' and pitch. Assuming small pitch angles, angle 'y' is approximately 90 degrees. Side BA equals approximately the product of 'pcslt' and pitch. Therefore, angle 'z' equals approximately 90 deg minus pitch minus 'pcang'. Side BC is the sum of 'pcran' and 'pcalt' times the sine of pitch. Side AC is determined using the law of cosines. Combining the law of sines and cosines, BCAN equals the inverse tangent of the following terms:

$$\frac{2.0 \text{ X BC X BA X } \sin(z)}{((AC)^2 + (BC)^2 - (BA)^2)} \qquad (1)$$

BCAN for negative pitch, (See Figure B.1(b)), is derived in a similar manner. Angle 'w' is known, using the small angle assumption, to be the sum of 90 degrees and 'pcang'. Sides BA and BC are known for similar reasons as given above. Therefore, angle BCAN for negative pitch equals the negative of Equation (1) above.

Knowing the pitch of the flight deck, ramp-crossing occurs when the following equation equals zero.

$$RAMP = \left| (Range + BC) - (pcran + x_f) \text{ X } \cos(BCAN) \right| \qquad (2)$$

In the simulation, because of integration step size considerations, if Equation (2) equalled some value between $\pm$ 6 feet, the time at which that value of Ramp occurred was designated as the ramp-crossing time. Height of hook at the ramp equalled the height of the aircraft c.g. referenced to the initial position of the ideal touchdown point minus the distance between aircraft c.g. and hook, as shown in Equation (3) below.

RALT = Altitude - (Range + BC) X tan(BCAN) - Deck Heave -HCGHK (3)

Time and position of the landing were recorded when the height of the aircraft main gear reached within $\pm$ 1 ft of the plane of the carrier deck. The main gear height equation is as follows:

HTMGTD = Altitude - (Range + BC) X tan(BCAN) - Deck Heave - (Distance between aircraft c.g. and main gear) (4)

Velocity of impact, as defined previously, equals the linear combination of aircraft sink rate and vertical velocity of the deck at the ideal touchdown point. The deck vertical velocity is measured assuming small pitch angles. Aircraft sink rate or velocity normal to the deck at point of impact was measured as shown in Figure B.2.

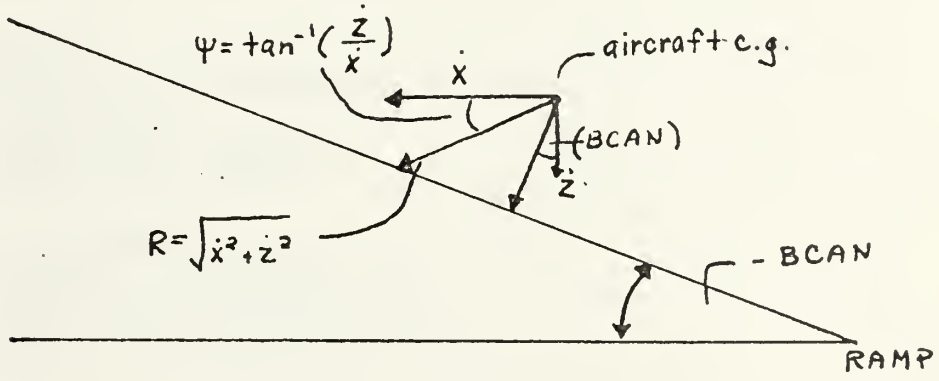

FIGURE B.2.

SINK RATE = R X cos(90/57.296 - (-BCAN) - ψ) or

= R X sin(-BCAN + ψ) (5)

INITIAL DISTRIBUTION LIST

		No. Copies
1.	Defense Documentation Center Cameron Station Alexandria, Virginia 22314	2
2.	Library, Code 0212 Naval Postgraduate School Monterey, California 93940	2
3.	Chairman, Department of Aeronautics Naval Postgraduate School Monterey, California 93940	1
4.	Assistant Professor R.A. Hess, Code 57 He Department of Aeronautics Naval Postgraduate School Monterey, California 93940	1
5.	Ens. Thomas M. Judd, USN 2749 Pelzer Avenue Montgomery, Alabama 36109	1
6.	Commander Naval Air Systems Command (PMA-235) Navy Department Washington, D.C. 20360	1
7.	Robert F. Ringland Senior Research Engineer, STI 13766 South Hawthorne Boulevard Hawthorne, California 90250	1

DOCUMENT CONTROL DATA - R & D

(Security classification of title, body of abstract and indexing annotation must be entered when the overall report is classified)

ORIGINATING ACTIVITY (Corporate author)
Naval Postgraduate School
Monterey, California 93940

2a. REPORT SECURITY CLASSIFICATION
Unclassified

2b. GROUP

REPORT TITLE

A Modified Design Concept, Utilizing Deck Motion Prediction, for the A-7E Automatic Carrier Landing System

DESCRIPTIVE NOTES (Type of report and inclusive dates)
Master's Thesis; (June 1973)

AUTHOR(S) (First name, middle initial, last name)

Thomas Maxwell Judd

REPORT DATE	7a. TOTAL NO. OF PAGES	7b. NO. OF REFS
June 1973	74	15

CONTRACT OR GRANT NO.

PROJECT NO.

9a. ORIGINATOR'S REPORT NUMBER(S)

9b. OTHER REPORT NO(S) (Any other numbers that may be assigned this report)

DISTRIBUTION STATEMENT

Approved for public release; distribution unlimited.

SUPPLEMENTARY NOTES

12. SPONSORING MILITARY ACTIVITY

ABSTRACT

The present concept of automatic carrier landings, Mode I operational capability, as employed in Navy carrier-based aircraft, was investigated. The aircraft chosen for study was the A-7E. The A-7E All Weather Carrier Landing System (AWCLS) and the carrier landing environment including burble effects and deck motion were simulated. Height of hook above ramp, touchdown point, and velocity of impact dispersions were determined. The current system was then modified, utilizing the concept of a SPN-42 Deck Motion Compensation Lead Computer which operates on the basis of known aircraft characteristics and predicted carrier heave motion. Simulation showed that automatic carrier landing performance as measured by number of ramp strikes, hard landings, and bolters could be improved. The modifications suggested require only a minimum of component additions to the AWCLS currently in use in the Navy.

KEY WORDS	LINK A		LINK B		LINK C	
	ROLE	WT	ROLE	WT	ROLE	WT
All-weather Carrier Landing System						
AN/SPN-42						
Approach Power Compensator System						
Automatic Flight Control System						
A-7E Aircraft						
Deck Motion Prediction						

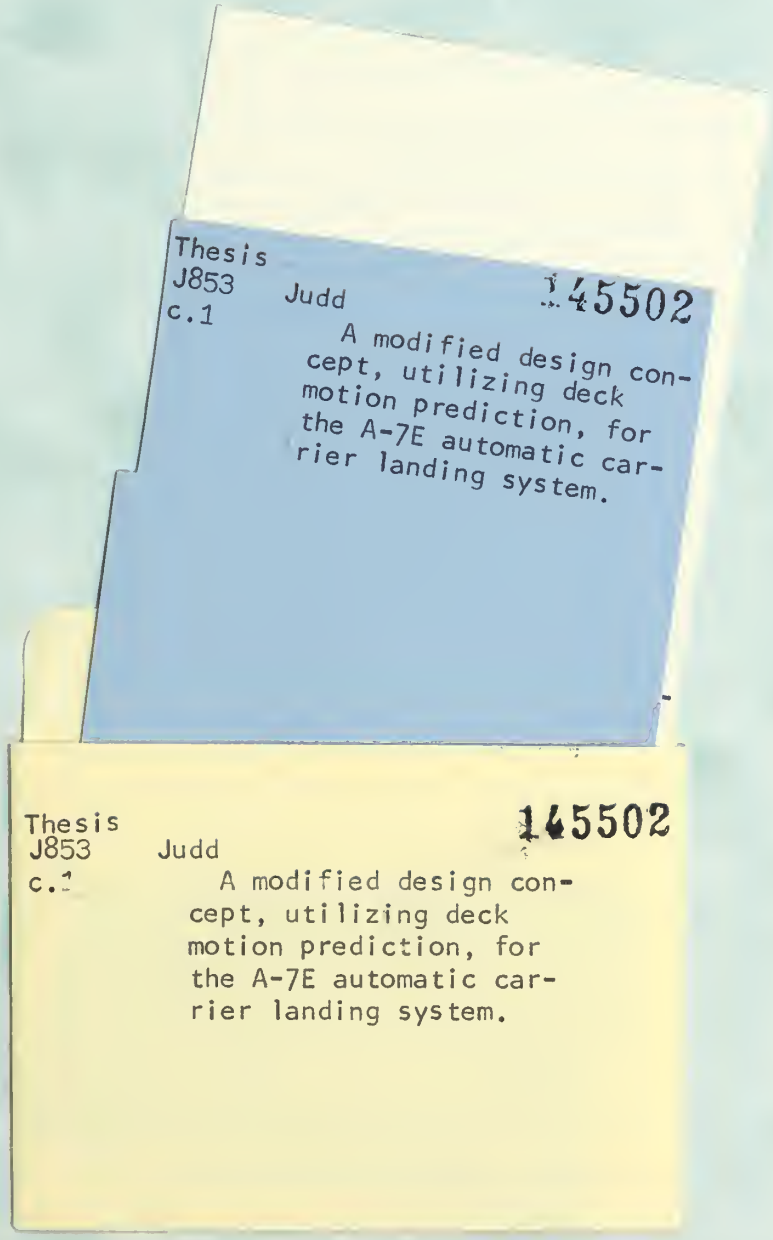

Thesis
J853
c.1
Judd
145502
A modified design concept, utilizing deck motion prediction, for the A-7E automatic carrier landing system.